UNIVERSIDAD DE CHILE
FACULTAD DE MEDICINA
ESCUELA DE POSTGRADO

ROLE OF mir-92a-3p IN THE EXPRESSION OF GENES OF CHEMORESISTANCE TO FLUOROURACIL AND OXALIPLATIN VIA ACTIVATION OF β-CATENIN IN COLON CANCER CELL LINES

PAULA ISABEL ESCALANTE ESCALANTE

TESIS PARA OPTAR AL GRADO DE DOCTOR EN CIENCIAS BIOMEDICAS

Directores de Tesis: Prof. Dr. Héctor R. Contreras Muñoz y Prof. Dr Luis A. Quiñones Sepúlveda

2022

UNIVERSIDAD DE CHILE
FACULTAD DE MEDICINA
ESCUELA DE POSTGRADO

INFORME DE APROBACION TESIS DE DOCTORADO EN CIENCIAS BIOMEDICAS.

Se informa a la Comisión de Grados Académicos de la Facultad de Medicina, que la Tesis de Doctorado en Ciencias Biomédicas presentada por el candidato

PAULA ISABEL ESCALANTE ESCALANTE

ha sido aprobada por la Comisión Informante de Tesis como requisito para optar al Grado de **Doctor en Ciencias Biomédicas** en Examen de Defensa de Tesis rendido el día 14 de diciembre de 2022.

Prof. Dr. Héctor R. Contreras M. y Prof. Dr. Luis A. Quiñones S.
Directores de Tesis
Dpto. de Oncología Básico-Clínica
Programa de Biología Celular y Molecular, ICBM
Facultad de Medicina, Universidad de Chile

COMISION INFORMANTE DE TESIS

PROF. DR. JUAN SEGURA

PROF. DR. MARCELO KOGAN

PROF. DRA. VERÓNICA BURZIO

PROF. DRA. LILIAN JARA
Presidente Comisión de Examen

TABLE OF CONTENTS

DEDICATORIA

“If you begin to regret, you’ll dull your future decisions and let others make your choices for you. Nobody can foretell the outcome. Each decision you make holds meaning only by affecting your next decision.”

– Erwin Smith

AGRADECIMIENTOS

En primer lugar, quisiera agradecer a mi tutor de tesis Dr. Luis Quiñones, quien me ha acompañado desde el inicio de mi camino por la Universidad de Chile. Gracias por haber confiado en mi potencial como estudiante desde el principio. A mi tutor Dr. Héctor Contreras, quien me mostro en sus clases la inspiración y el entusiasmo por enseñar la ciencia. A ambos les agradezco por haber creído en mí, incluso en muchas ocasiones más de lo que yo he creído en mí misma. Por acompañarme ambos en este camino no solo como docentes, si no como guías y padres que nunca tuve, pese a todas las dificultades que se presentaron en mi camino durante mis estudios de postgrado. Gracias por hacerme sentir parte de una familia, y aunque este lejos, nunca olvidare todo lo que han hecho por mí.

A mis compañeros del Laboratorio de Carcinogénesis Química y Farmacogenética, gracias por estar conmigo durante el arduo trabajo de la Red de Laboratorios Universitarios de Diagnóstico COVID-19 durante el año 2020-2021. Trabajar con ustedes me ha hecho sentir que he cumplido con el propósito de un profesional de la salud durante los tiempos difíciles de pandemia. A Leslie Cerpa y Alejandra Lavanderos, por ser excelentes líderes del equipo. A Salvador Quiroz, Eduardo Lamoza, Daniela Poblete, Christopher Sandoval, y a todos quienes formaron parte del excelente equipo de laboratorio, que hicieron que las largas tardes de trabajo fueran más amenas. Por último, a Don Michel Muñoz, por su arduo y dedicado trabajo, y por ser siempre una buena compañía.

A mis compañeros del Laboratorio de Oncología Celular y Molecular, también les agradezco por apoyarme durante el desarrollo de mi tesis. A Graciela Caroca, por mantener el laboratorio siempre en marcha, y también por tener un gran corazón y hacerme sentir siempre como en casa. A Sebastián Indo, María José Torres, Fernanda López, Sebastián Troncoso por estar ahí en cada paso de mi tesis, apoyarme en el desarrollo de mis experimentos y estar ahí para ayudarme a no meter la pata. Los quiero mucho y voy a extrañarlos a todos, y espero que me recuerden en cada gato que dibujé por ahí.

También quisiera agradecer a mi comisión de tesis por ayudarme con cada una de sus experiencias profesionales. A la doctora Lilian Jara, por su trabajo y guía como Tutora Académica, a la Dra. Verónica Burzio por ser un apoyo primordial en el diseño experimental de mi proyecto de Tesis. A los doctores Juan Segura y Marcelo Kogan por aportarme con su inmenso saber y hacer de este trabajo la mejor versión que podría ser.

Por último, quisiera agradecer a las personas que han estado conmigo siendo un apoyo incondicional en mi vida. A mi suegrita Sandra Retamal, mi cuñada Rossana Améstica, mi suegro Eduardo Améstica, por haberme acogido como parte de su familia. A Claudia Quintana por compartir conmigo múltiples momentos, y ser una persona genuina y capaz de alegrarme en los días más difíciles. A mis amigos Carlos Donoso, Madelaine Bao y Paula Calvo, son los mejores amigos que una rarita como yo podría desear. Siempre estarán en mi corazón, aunque estemos a kilómetros de distancia. Y a mi esposo Felipe Améstica, eres mi pilar, mi compañero de vida y el que me hace reír todos los días. Migrar no es fácil, pero a tu lado siento que podría recorrer el mundo. Gracias por enseñarme el amor incondicional, ser el mejor padre de nuestros gatos, y el mejor esposo del mundo.

RESUMEN

El cáncer colorrectal (CCR) es el segundo más diagnosticado en Chile y el mundo. El tratamiento de primera línea del CCR metastásico consiste en la asociación de 5-fluorouracilo (5-FU) y oxaliplatino (L-OHP), conocido como el esquema de quimioterapia FOLFOX. Sin embargo, la tasa de supervivencia a 5 años es inferior al 14% para pacientes que debutan con metástasis a distancia no resecables, atribuido principalmente al desarrollo de quimiorresistencia. Se ha informado de que miR-92a-3p induce transición epitelial-mesenquimal (TEM), disminuye la sensibilidad *in vitro* a 5-FU y L-OHP a través de la activación de β-catenina, y promueve quimiorresistencia en modelos animales. Los genes biomarcadores de respuesta a quimioterapia FOLFOX incluyen dihidropirimidina deshidrogenasa (*DPYD*), timidilato sintasa (*TYMS*), metilentetrahidrofolato reductasa (*MTHFR*) y los genes codificantes para las subunidades de reparación de ADN *ERCC1*, *ERCC2* y *XRCC1*. Las regiones promotoras de estos genes contienen elementos de respuesta para factores de transcripción asociados a β-catenina y a TEM, y la sobreexpresión de *DPYD*, *TYMS* y *ERCC1* ha mostrado ser desencadenada por TEM. Sin embargo, la relación entre miR-92a-3p, la activación de β-catenina, la expresión de estos genes biomarcadores, y la quimiorresistencia de las células tumorales al tratamiento FOLFOX aún no ha sido explorada.

En esta investigación exploramos el papel de miR-92a-3p en la activación de TEM en células tumorales, si esto incrementa la expresión de *DPYD*, *TYMS*, *MTHFR*, *ERCC1*, *ERCC2* y *XRCC1* a través de la activación de β-catenina induciendo resistencia de células tumorales de CCR al tratamiento con 5-FU y L-OHP. Para comprobar esta hipótesis en un modelo *in vitro*, transfectamos las líneas celulares de cáncer de colon SW480 y SW620 con *mimics* e inhibidores de miR-92a-3p en experimentos independientes. Cuantificamos la expresión de *DPYD*, *TYMS*, *MTHFR*, *ERCC1*, *ERCC2* y *XRCC1* y evaluamos la activación de β-catenina y TEM en cada experimento. Paralelamente, se realizaron pruebas de quimiosensibilidad *in vitro* de las líneas celulares al tratamiento con FOLFOX.

En resumen, nuestros hallazgos mostraron que el aumento o la disminución transitoria de miR-92a-3p no conduce a la activación de β-catenina en nuestros experimentos, ni al aumento de la expresión de *DPYD*, *TYMS*, *MTHFR*, *ERCC1*, *ERCC2* y *XRCC1* durante el tiempo de transfección. Por lo tanto, no podemos confirmar que miR-92a-3p tenga un papel relevante en la activación de la transición epitelial-mesenquimal y la quimiosensibilidad *in vitro* de FOLFOX en líneas celulares de cáncer de colon.

ABSTRACT

Colorectal cancer (CRC) is the second most frequently diagnosed cancer in Chile and worldwide. First-line treatment of metastatic CRC consists mainly of the association of 5-fluorouracil (5-FU) and oxaliplatin (L-OHP), known as the FOLFOX scheme. Despite the advances in CRC treatment, the 5-year survival rate for patients debuting with non-resectable distant metastasis is lower than 14%, attributed mostly to the development of chemoresistance. It has been reported that miR-92a-3p induces epithelial-mesenchymal transition (EMT), contributing to tumor progression in tumor cells via activation of β-catenin. Furthermore, increased miR-92a-3p decreases *in vitro* 5-FU and L-OHP sensitivity and promotes chemoresistance in animal models. Biomarker genes that impact the response to FOLFOX therapy include dihydropyrimidine dehydrogenase (*DPYD*), thymidylate synthase (*TYMS*), methylenetetrahydrofolate reductase (*MTHFR*), and the genes encoding the DNA repair subunits *ERCC1*, *ERCC2*, and *XRCC1*. The promoter regions of these genes contain response elements for transcription factors associated with β-catenin and EMT, and overexpression of the genes *DPYD*, *TYMS*, and *ERCC1* can be triggered by EMT. Regardless, the relationship between miR-92a-3p, activation of β-catenin, expression of the genes *DPYD*, *TYMS*, *MTHFR*, *ERCC1*, *ERCC2*, and *XRCC1*, and resistance of tumor cells to FOLFOX chemotherapy has not been previously explored.

In this research, we explored the role of miR-92a-3p in the promotion of EMT in tumor cells, the upregulation of *DPYD*, *TYMS*, *MTHFR*, *ERCC1*, *ERCC2*, and *XRCC1* expression via activation of β-catenin and whether it led to resistance of CRC tumor cells to treatment with 5-FU and L-OHP. To test this hypothesis in an in-vitro model, we transfected the colon cancer cell lines SW480 and SW620 with miR-92a-3p mimics and miR-92a-3p inhibitors in independent experiments. We quantified the expression of the *DPYD*, *TYMS*, *MTHFR*, *ERCC1*, *ERCC2*, and *XRCC1* genes and the activation of β-catenin and EMT in each experimental setting. In parallel, *in vitro* chemosensitivity tests of cell lines to FOLFOX treatment were performed.

In summary, our findings did not show that transient increase or decrease of miR-92a-3p led to activation of β-catenin and EMT in our experimental settings, nor the expression of *DPYD*, *TYMS*, *MTHFR*, *ERCC1*, *ERCC2*, and *XRCC1* during the time of transfection. Therefore, we cannot confirm that miR-92a-3p has a role in the activation of epithelial-mesenchymal transition and FOLFOX *in vitro* chemosensitivity in colon cancer cell lines.

THEORETICAL FRAMEWORK

Colorectal cancer (CRC) is, to date, still one of the leading causes of death in Chile and worldwide, and it is defined as malignant neoplasia that develops from the colon or rectum epithelial tissue[1–3]. A higher incidence of CRC is observed in developing countries with increasing Human Developed Index (HDI) characterized by higher prevalence of risk factors such as obesity, low physical activity, and low socioeconomic status[3,4]. According to the records of the Chilean Ministry of Health (Ministerio de Salud de Chile), CRC mortality increased a 19.3% between the years 2000 and 2013 and was the fourth cause of years of life lost due to disability (YLD) by the year 2013[5,6]. These statistics show that CRC is a severe burden to our country and healthcare providers, and because of our current economic growth rate, we should expect an increase in mortality and morbidity due to CRC in the future.

The CRC stage is determined depending on the degree of invasion of the tumor into the colon tissue, lymph nodes, and local and distant organs[3,5–7]. Early-stage CRC (stage I to II) is most often treated by resection of the tumor and, in most cases, does not require adjuvant chemotherapy. Stage III CRC implies invasion of lymph nodes, and stage IV implies metastasis to distant organs, commonly the liver and lungs. Patients diagnosed with stages III and IV require neoadjuvant, adjuvant, or palliative chemotherapy and prognosis depends mainly on the viability of eventually achieving surgical tumor resection[3,5].

Chemotherapy of colorectal cancer

5-Fluorouracil (5-FU) based chemotherapies are the foundation of current CRC treatment, from which FOLFOX consists of the association of 5-FU, leucovorin (LV), and oxaliplatin (L-OHP), while FOLFIRI is based on the combination of 5-FU, LV, and irinotecan. Moreover, triplet chemotherapy schemes consisting of 5-FU, L-OHP, and irinotecan, plus LV (FOLFOXIRI) have also shown to be effective, significantly outperforming the clinical response observed with each of these chemotherapeutic drugs in monotherapy. Capecitabine, a prodrug metabolized into 5-FU, is also part of the 5-FU-based chemotherapy schemes. In Chile, the FOLFOX chemotherapy scheme is considered the first-line treatment for advanced mCRC[3,5,8–10]

Improved guidelines for screening, diagnostic and novel biological therapies have improved the survival rate of patients diagnosed with local and regional CRC (stages I, II, III)

during the last 50 years. Current 5-year survival percentages in patients diagnosed with localized CRC (90%) and regional mCRC (71%) indicate a positive trend. In contrast, patients diagnosed with distant (stage IV) metastatic CRC (mCRC) face a less optimistic outlook. For patients debuting with distant mCRC, the 5-year survival percentage is still only 14%, despite the efforts that have improved survival in the other groups of patients.

Targeted therapies, including anti-EGFR (cetuximab) and antiangiogenic (bevacizumab) monoclonal antibodies, aim to improve survival in this group of patients and are increasingly being included as part of the first-line treatment of stage IV CRC in developed countries, but in Chile and other developing countries (where CRC incidence has shown to be rising) these treatments signify a heavy burden for healthcare providers and therefore are reserved as a second-line treatment[2,3,9,10]. In addition, a significant correlation between low socioeconomic status and a higher risk of being diagnosed with high-stage disease further confirms that vulnerable populations suffer the heaviest toll from mCRC[2,3].

One of the main factors involved in the low survival rate of patients diagnosed with advanced mCRC is the rapid development of acquired resistance to the foundational 5-FU-based chemotherapy schemes[2,11]. Exploring the signaling pathways that enable cancer cells to persist the cytotoxic treatment could help us to assess and predict which patients will be at higher risk of therapeutic failure, in the same manner as we currently screen for other specific mutations in patients that receive targeted therapies, tailoring the chemotherapeutic scheme to improve the rate of therapeutic success in patients with advanced mCRC, and hopefully, develop new strategies that address chemoresistance[12].

The role of EMT and mir-92a-3p in tumor progression and chemoresistance

Epithelial-mesenchymal transition (EMT) and mesenchymal-epithelial transition (MET) are physiological processes that enable cellular plasticity and adaptability and generally have a role during specific steps of embryonic development and wound healing. Briefly explained, EMT occurs when a cell characterized by an epithelial phenotype (including cell morphology, polarity, and expression of cell-to-cell and cell-to-extracellular matrix adhesion molecules) undergoes a gradual transformation to acquire a mesenchymal phenotype. In contrast, MET implies the opposite process, when a cell with a mesenchymal phenotype (characterized by low expression of adhesion proteins and an elongated, non-polarized fibroblastic morphology) will gradually acquire or recover these epithelial characteristics[13–16].

Tumor cells that acquire a mesenchymal phenotype through the execution of the EMT program gain traits that are relevant in the process of metastasis, including downregulation of the expression of cell adhesion molecules, detachment from surrounding cells, and increased cell motility and invasiveness. Conversely, once these migratory mesenchymal tumor cells arrive at an acceptive stroma, they may undergo MET, allowing these invasive cells to re-express adhesion molecules and recover their proliferative rate, consolidating new colonies that eventually will evolve into a clinically relevant metastatic focus. Indeed, EMT and MET are not definitive processes, and cancer cells can exist at distinct points on the epithelial-mesenchymal spectrum at different time points of disease progression. Because of their role in enabling migration, invasiveness, and colonization of metastatic niches, EMT and MET are pivotal during cancer progression and are frequently active in metastatic disease[13–16].

EMT is mainly governed by a set of transcription factors, including *SNAIL*, *SLUG*, *ZEB1/2*, and *TWIST1*, which regulate the expression of several genes that unfold the multiple steps of the transition. These EMT-transcription factors (EMT-TFs) have a prominent role in embryonic development, but their expression is highly downregulated in well-differentiated cells, except for cells under inflammation and during neoplastic processes[14,16,17].

In this regard, adherens junctions are characteristic structures of epithelial cells, a form of cell-to-cell interactions comprised, among other proteins, of the epithelial biomarker E-cadherin and β-catenin, a protein that aids in scaffolding E-cadherin to the actin cytoskeleton. One of the best-described processes triggering EMT is the activation of β-catenin. Active β-catenin (ABC) dislodges from the adherens junction and translocates to the cell nucleus, where it interacts with T-cell factor (TCF)/Lymphoid enhancer-binding factor (Lef) transcriptions factors, increasing the expression of β-catenin target genes, including several oncogenes and EMT-TFs, promoting the initiation of EMT in the tumor cell[18–20].

Current evidence has revealed that tumor cells, rather than function as independent entities, are deeply influenced by the tumor microenvironment. In this regard, cancer-associated fibroblasts (CAFs) have shown to be essential components of the tumor microenvironment that, unlike normal fibroblasts, support tumor progression and metastasis[21,22]. The research by Hu *et al.* (2019)[23] reported that exosome communication of CAFs with colorectal cancer tumor cells increases migration, invasiveness, and chemoresistance to combined treatment with 5-FU and L-OHP in colon cancer cell lines. Their findings highlighted a specific microRNA upregulated in CAF-derived exosomes compared to normal fibroblast-derived exosomes: mir-92a-3p. This specific microRNA has been reported to

act as an oncomiR, a microRNA that behaves like an oncogene, promoting tumor initiation and progression.

MiR-92a-3p has been reported to promote EMT in tumor cells through downregulation of PTEN, a tumor suppressor, FBXW7, a subunit of the SCF ubiquitin ligase complex that participates in proteasomal degradation of several proteins involved in mitogenic pathways, and has shown to promote migration and invasiveness by directly targeting E-cadherin[23–28]. Downregulation of both PTEN and FBXW7 has been associated with activation of β-catenin [23,25,29,30]. Moreover, confocal microscopy images have revealed that expression of mir-92a-3p in tumor cells leads to increased β-catenin in the nuclear fractions of tumor cells, which suggests that this microRNA may activate β-catenin, leading to an increased expression of β-catenin target genes[23]. Nevertheless, the mechanism by which miR-92a-3p affects the response to FOLFOX chemotherapy schemes in colon cancer cells has not been fully elucidated.

Biomarkers of response in chemotherapy of colorectal cancer

Because of the narrow therapeutic window of FOLFOX and other 5-FU-based chemotherapy schemes, significant efforts are being made to profile the diverse array of adverse events and therapeutic responses observed in populations of CRC patients under chemotherapy[31]. The scope of pharmacogenomic research is to define the genetic variants that explain this high inter-individual variance of responses to pharmacotherapy within human populations, aiming to define guidelines to tailor the best therapeutic strategy for each patient[32–34].

In the process, pharmacogenomic research has identified a remarkable set of genes that have shown to impair or modify the response and toxicity profiles to FOLFOX chemotherapy in mCRC patients. These biomarker polymorphisms are often found in genes that have a specific role in FOLFOX pharmacodynamics and pharmacokinetics[31].

Pharmacogenomic Biomarkers of Fluorouracil Response

5-FU is one of the oldest and most widely used chemotherapy tools in the fight against cancer. It is classified as an antimetabolite, meaning that it exerts its cytotoxic effect by inhibiting biochemical processes in the cancer cell.

Because of its structural similarity to the pyrimidine uracil, 5-FU is rapidly transported and metabolized in the cell into active and inactive metabolites, from which 5-fluoro-2′-deoxyuridine 5′-monophosphate (FdUMP) is the major active one. Thymidylate synthase (*TYMS*) is an enzyme that catalyzes the synthesis of thymidine monophosphate from its precursor deoxyuridine monophosphate, requiring 5,10-methylenetetrahydrofolate (methylene-THF) as a methyl group-donor in the reaction. FdUMP inhibits *TYMS*, impairing the balance of deoxynucleotide levels and DNA replication, leading to cell cycle arrest (**Figure 1**)[9,31,35–37].

Being the main therapeutic target of 5-FU, *TYMS* has an essential role in 5-FU-based chemotherapy response. Indeed, polymorphic variants in the promoter enhancer region of the *TYMS* gene, associated with increased protein expression, have been linked with decreased survival in CRC patients treated with 5-FU-based chemotherapy, establishing this gene as a biomarker for FOLFOX response[9,31,35].

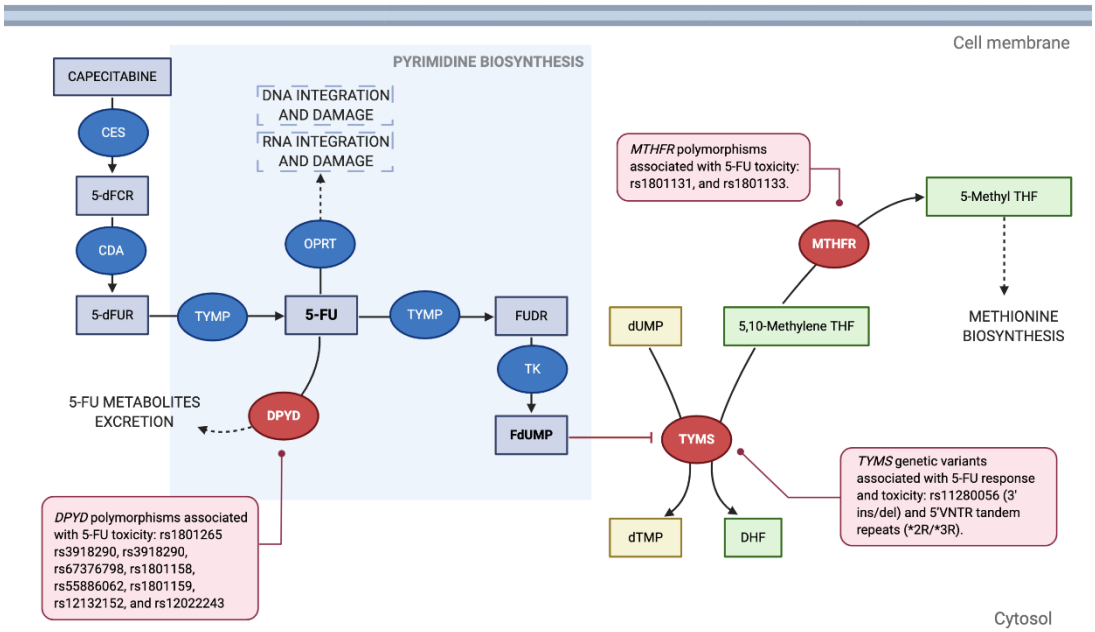

Figure 1. Mechanism of action of 5-fluorouracil: Capecitabine is a prodrug that is converted to 5-FU through metabolization by the enzymes carboxylesterase (CES) into 5'-deoxy-5-fluorocytidine (5′-dFCR), then by cytidine deaminase (CDA) into doxifluridine (5′-dFUR), and finally by thymidine phosphorylase (TYMP) into 5-FU. 5-FU is metabolized by TYMP into floxuridine (FUDR), and then by thymidine kinase (TK) into 5-fluoro-2′-deoxyuridine 5′-monophosphate (FdUMP), which inhibits its main therapeutic target thymidylate synthase (*TYMS*) by competing with its natural ligand deoxyuridine monophosphate (dUMP). *TYMS* normally transfers methyl groups from 5-10-methylenetetrahydrofolate (5,10-methylene THF) into dUMP to obtain deoxythymidine monophosphate (dTMP) and dihydrofolate (DHF), which is the rate-limiting step in the synthesis of deoxythymidine nucleotides required for DNA replication. 5-FU can be directly inactivated by dihydropyrimidine dehydrogenase (*DPYD*) into metabolites that are eliminated.

Binding of FdUMP to *TYMS* is stabilized by 5,10-methylene THF, and metabolization of this cofactor into 5-methyltetrahydrofolate (5-methyl THF) by methylenetetrahydrofolate reductase (*MTHFR*) reduces FdUMP affinity to *TYMS*. 5-FU can also be metabolized by orotate phosphoribosyltransferase (OPRT) into 5-FU metabolites that are incorporated into the RNA and DNA of the cell, accounting to a lesser extent for 5-FU cytotoxicity. Polymorphisms of *DPYD*, *TYMS*, and *MTHFR* coding genes have been associated with 5-FU response [31]. Enzymes are shown as ovals and metabolites as rectangles. Image and figure description from Escalante *et al*. (2021)[12]. Created with BioRender.com.

5-FU is associated with LV (also known as folinic acid) in almost all 5-FU-based chemotherapy schemes because inhibition of *TYMS* by FdUMP requires the formation of a ternary complex that is stabilized by the binding of methylene-THF, a folate metabolite. However, methylene-THF can also be depleted by the enzyme methylenetetrahydrofolate reductase (*MTHFR*), diverting folates to the methionine biosynthesis pathway and decreasing the affinity of FdUMP to *TYMS*[31,35,38]. Because of the relevance of *MTHFR* expression in FOLFOX response, some polymorphisms of this gene are considered potential biomarkers of 5-FU-based chemotherapy[35].

Up to 85% of 5-FU is metabolized by the enzyme dihydropyridine dehydrogenase (DPD) into the inactive metabolite 5,6-dihydro-5-fluorouracil. Polymorphisms of the *DPYD* gene encoding DPD, have been associated with low or null enzymatic activity, leading to accumulation of 5-FU and thus increased risk of toxicity[31,36,38]. Overall, these findings imply that expression of the genes *DPYD*, *TYMS* and, *MTHFR* have an impact on sensitivity of tumor cells to 5-FU.

Pharmacogenomic Biomarkers of Oxaliplatin Response

Oxaliplatin is a cytostatic drug from the group of platinum derivatives. Its mechanism of action is based on the high reactivity of the platinum moiety with biomolecules in the cell, particularly with DNA nucleotides. The platinum inter-strand and intra-strand crosslinks interfere with DNA replication and transcription, leading to DNA damage and overall triggering apoptotic pathways of the affected cell. Nonetheless, tumor and normal cells have mechanisms to withstand the damage induced by platinum derivatives, including two major pathways, the nucleotide excision pathway (NER) and the base excision pathway (BER)[11,38–41].

NER is the main pathway involved in the repair of platinum-DNA adducts, and it is performed by several protein complexes that recognize the damage, excise a large region of the affected DNA strand, and synthesize a new strand filling the gap in the genetic material. The BER pathway may also, to a lesser extent, participate in the repair process of platinum-

DNA adducts through a different mechanism that involves the cleavage of the altered base, synthesis, and ligation of the repaired DNA strand (**Figure 2**)[31,38–43].

Polymorphisms in genes coding for the *ERCC1*, *ERCC2* (from the NER pathway), and *XRCC1* (from the BER pathway), have been studied as biomarkers of both response and toxicity of FOLFOX regimens due in part to the fact that overexpression or gain of function of these proteins can inhibit platinum-derived DNA damage and DNA damage-mediated apoptosis[31,38,39,44].

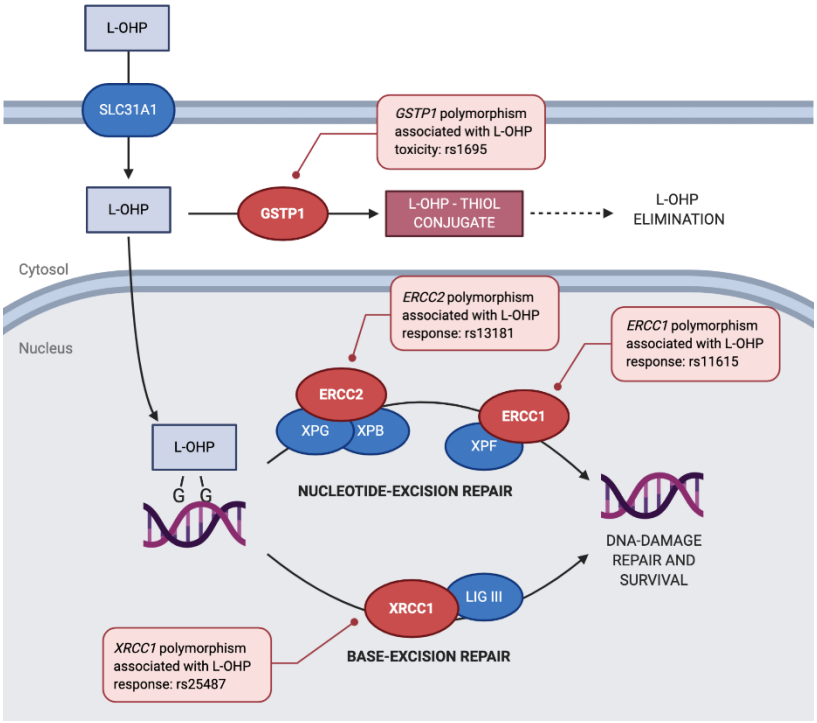

Figure 2. Mechanism of action of Oxaliplatin: L-OHP is transported into the cell by solute carrier family 31 (copper transporter), member 1 (SLC31A1). Inside the cell, L-OHP forms adducts with the DNA, in particular with guanine bases, forming DNA crosslinks that induce apoptosis of the cell. Platinum-DNA adducts can be repaired by the nucleotide-excision repair pathway (NER), which involves several steps and enzyme complexes, including xeroderma pigmentosum, complementation group G (XPG) which interacts with the TFIIH core complex helicase, composed by the excision repair cross-complementation group 2 (*ERCC2*) and xeroderma pigmentosum group B-complementing protein (XPB), unwinding the damaged DNA strand. This step is followed by an excision step of the damaged DNA fragment catalyzed by the endonuclease complex formed by the excision repair cross-complementation group 1 (*ERCC1*) and xeroderma pigmentosum, complementation group F (XPF), which is followed by the synthesis of a new DNA strand. Alternatively, platinum-DNA adducts can be repaired by the base-excision repair pathway (BER), in which the last step involves the binding of DNA 5′ and 3′ ends by the participation of X-ray repair cross-complementing 1 (*XRCC1*) and DNA ligase III (Lig III). Both pathways lead to the elimination of platinum-DNA adducts inhibiting DNA damage-driven apoptosis. L-OHP can be directly detoxified by glutathione S-transferase π 1 (GSTP1) into L-OHP-thiol conjugates that are eliminated. Polymorphisms of *ERCC1*, *ERCC2*, *XRCC1*, and *GSTP1* coding genes have been associated with L-OHP response[31]. Several enzyme complexes from the NER and BER

pathways are omitted for simplicity. Enzymes are shown as ovals and metabolites as rectangles. Image and figure description from Escalante *et al*. (2021)[12]. Created with BioRender.com.

EMT, biomarker genes, and the potential role of miR-92a-3p

As we have previously discussed, the role of EMT in cancer progression and drug resistance has been well researched since it was proposed in the '90s. Although several mechanisms, like the expression of multidrug resistance efflux transporters, cancer stem cells, and activation of mitogenic pathways, are considered prominent contributors to this acquired chemoresistance, what happens with the expression of FOLFOX biomarker genes during EMT has not yet been extensively studied[12,45].

In this context, previous research has shown a significant correlation between EMT and overexpression of *DPYD* and *TYMS* in hepatocellular carcinoma patient samples, lung cancer cells, colon cancer cells, and other cell lines[46–49]. Furthermore, *TWIST1* silencing has shown to downregulate *DPYD* and *TYMS* expression in colon cancer cell lines *in vitro*, while *DPYD* knockdown inhibits *TWIST*-induced EMT in breast cancer-derived mammospheres, and *TYMS* overexpression upregulates *ZEB1* colon cancer cell lines[47,48,50]. These findings suggest that EMT-mediated tumor progression has a strong impact on chemosensitivity to 5-FU through upregulation of *DPYD* and *TYMS* expression.

EMT-TFs, including *SNAIL*, *SLUG*, and *ZEB1/ZEB2*, have shown to induce overexpression of *ERCC1* in colon cancer, head and neck cancer, and non-small cell carcinoma cell lines *in vitro*, which correlates with resistance to platinum derivates[51–53]. These results indicate a strong relationship between the EMT program, *ERCC1* expression, and L-OHP resistance.

On the contrary, recent evidence suggests that EMT seems to correlate with the downregulation of *XRCC1*. Expression of E-cadherin and *XRCC1* is upregulated by hsa_circ_0012563, a tumor suppressor circular RNA, in esophageal squamous cell carcinoma (ESCC) cell lines, while N-cadherin, a mesenchymal biomarker, is downregulated[54].

Changes in the expression profile of these biomarker genes may be necessary to adapt to the modified metabolic requirements of cancer cells, forming part of the process recently described as metabolic reprogramming[12,16]. Indeed, *TYMS* and *DPYD* are enzymes of the pyrimidine biosynthesis pathway, and *MTHFR* participates in the metabolism of folates, which may be dysregulated during cancer progression to cope with increased proliferative activity,

and may explain why overexpression of the genes *TYMS* and *DPYD* seems to be required during EMT in experimental settings[12,47,48]. Similarly, overexpression of enzymes of the NER pathway, including *ERCC1* and *ERCC2*, may be overexpressed to compensate for increased replicative stress in proliferative cancer cells as part of this metabolic reprogramming. Overall, previous research suggests that the genes *DPYD*, *TYMS*, and *ERCC1*, are upregulated during the EMT program, and this phenomenon may also upregulate the expression of the genes *MTHFR*, *ERCC2*, and *XRCC1*.

As we discussed in our recent publication, the human promoter regions of *DPYD*, *TYMS*, *MTHFR*, *ERCC1*, *ERCC2*, and *XRCC1* contain response elements to EMT-transcription factors, which include *SLUG*, *ZEB1*, *TWIST1*, β-catenin/TCF3, and β-catenin/TCF4, suggesting that these genes may be affected by the EMT process occurring during tumor progression[12]. Based on the collected evidence, we propose that the expression of the genes *DPYD*, *TYMS*, *MTHFR*, *ERCC1*, *ERCC2*, and *XRCC1* may be modulated by EMT-TFs, and β-catenin/TCF3/4 transcription factor complexes, and therefore, may be affected by mir-92a-3p, leading to FOLFOX chemoresistance in colon cancer cells, as we explain in **Figure 3.**

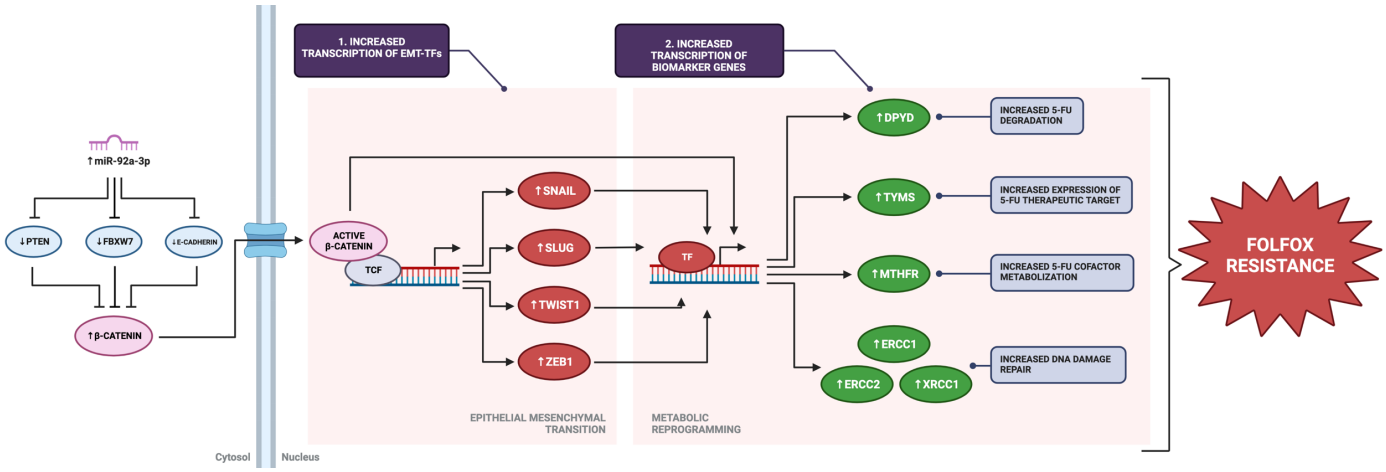

Figure 3. Proposed role of miR-92a-3p in the response to FOLFOX chemotherapy: 1.- mir-92a-3p activates β-catenin through previously explored mechanisms, upregulating transcription of epithelial-mesenchymal transition-transcription factors (EMT-TFs), triggering epithelial-mesenchymal transition (EMT) in cancer cells. 2.-EMT-TFs *SNAIL*, *SLUG*, *TWIST1*, and *ZEB1* directly upregulate transcription of FOLFOX biomarker genes as part of metabolic reprogramming, allowing adaptation of the cancer cell to increased proliferation and replication stress. These metabolic changes triggered by progressive EMT in cancer cells affect FOLFOX response by increasing 5-FU and L-OHP elimination (*DPYD*), increasing expression of 5-FU therapeutic target (*TYMS*), decreasing levels of 5,10-methylene THF required for proper *TYMS* inhibition (*MTHFR*), and increasing DNA damage repair inhibiting DNA damage-driven apoptosis (*ERCC1*, *ERCC2*, *XRCC1*). Overall, this would lead to FOLFOX resistance. Adapted from Escalante *et al.* (2021)[12].

Over the last years, it has been assumed that tumor cells that exhibit a mesenchymal phenotype are inherently more resistant to chemotherapy compared to tumor cells with a well-differentiated epithelial phenotype. This phenomenon has been attributed to their reduced proliferative activity and the expression of efflux transporters, such as the ATP-binding cassette family proteins, but the precise mechanism of resistance is lesser-known. In this research, we aimed to establish the role of a specific oncomiR, mir-92a-3p, in the activation of the EMT program in tumor cells and the impact of this phenomenon on the expression of genes that predict FOLFOX chemotherapy response, which may constitute an underexplored mechanism of chemoresistance in tumor cells that undergo EMT.

HYPOTHESIS

MiR-92a-3p promotes epithelial-mesenchymal transition in SW480 and SW620 colon cancer cells, upregulating the expression of *DPYD*, *TYMS*, *MTHFR*, *ERCC1*, *ERCC2*, and *XRCC1* via activation of β-catenin, which ultimately leads to resistance of CRC tumor cells to treatment with 5-FU and L-OHP.

RESEARCH AIM

The aim of this study is to determine whether activation of β-catenin induced by miR-92a-3p upregulates the expression of *DPYD*, *TYMS*, *MTHFR*, *ERCC1*, *ERCC2*, and *XRCC1* genes, and activates EMT in SW480 and SW620 colon cancer cell lines, reducing *the in vitro* sensitivity to treatment with 5-FU and L-OHP.

SPECIFIC OBJECTIVES

1. To evaluate the effect of miR-92a-3p on activation of β-catenin and EMT in SW480 and SW620 cell lines.
2. To determine whether activation of β-catenin by miR-92a-3p upregulates the *in vitro* expression *DPYD*, *TYMS*, *MTHFR*, *ERCC1*, *ERCC2*, and *XRCC1* in SW480 and SW620 cell lines.
3. To determine the effect of upregulation of *DPYD*, *TYMS*, *MTHFR*, *ERCC1*, *ERCC2*, and *XRCC1* induced by miR-92a-3p on *in vitro* chemosensitivity to 5-FU and L-OHP treatment in SW480 and SW620 cell lines.

METHODOLOGY

Research objective 1: Effect of miR-92a-3p on activation of β-catenin and EMT *in vitro*

To study the activation of EMT mediated by miR-92a-3p, we worked with two types of human colon cancer cell lines, SW480 derived from a primary tumor (ATCC® CCL-228TM) and SW620 derived from a lymph node metastasis (ATCC® CCL-227TM). Cells were cultured at 37 °C and without CO_2 in Leibovitz's L-15 culture medium supplemented with 10% fetal bovine serum (FBS), according to the instructions from the manufacturer. For protein RNA and protein extraction we seeded 50,000 cells per well in 12 well plates and 20,000 cells per well in 24 well plates for immunofluorescence assays and cultured them until 60% confluence before transfection.

We transfected SW480 and SW620 cells with increasing concentrations of mirVana™ miR-92a-3p-mimic, which consists of a single-stranded RNA oligonucleotide that mimics the activity of a specific miR, or a corresponding mirVana™ mimic negative control oligonucleotide at equal concentrations (1 nM, 5 nM, 10 nM, and 20 nM) using Lipofectamine 2000™ 1 µL/mL for 24 hours before RNA extraction. Cell lines were cultured at 37 °C with 5% CO_2 in Opti-MEM™ reduced serum medium during transfection.

On the opposite, we transfected the cell lines with 100 nM mirVana™ miR-92a-3p-inhibitor, which consists of a single-stranded RNA oligonucleotide that is complementary to miR-92a-3p, inhibiting its activity, or a corresponding mirVana™ inhibitor negative control oligonucleotide at equal concentrations using increasing concentrations of Lipofectamine 2000™ reagent (2, 2.5, and 3 µL/mL) for 24 hours before RNA extraction. Cell lines were cultured at 37 °C with 5% CO_2 in Opti-MEM™ reduced serum medium during transfection.

Once the optimal concentration of mimics and inhibitors was established, the expression of EMT-transcription factors *SNAIL*, *SLUG*, *ZEB1*, and *TWIST1,* as well as levels of E-Cadherin, N-Cadherin, and Vimentin mRNA was quantified in SW480 and SW620 transfected with the miR-mimic, inhibitor, or corresponding control by RT-qPCR. Primer sequences are specified in Appendix 1. We also extracted proteins from transfected cells and quantified the proteins of the genes that were up or downregulated in any of the transfection conditions by Western blot. Antibodies used for western blot are specified in Appendix 2.

To explore the role of miR-92a-3p expression in the activation of β-catenin and ABC, we measured both forms of β-catenin in SW480 and SW620 cells transfected with miR-92a-3p

mimic or inhibitor by Western blot with specific antibodies. Subcellular location of β-catenin was assessed in transfected cells by immunofluorescence microscopy, and as a positive and negative control, SW480 and SW620 cell lines were treated with the Wnt pathway activator SB-216763 10 μM to induce canonical Wnt/β-catenin signaling, or with the Wnt inhibitor IWR-1-endo 10 μM to inhibit Wnt/β-catenin signaling, as performed in previous experimental settings[55–58].

In these experiments, we expected to find an increment in the levels of expression of EMT-TFs, N-Cadherin, and Vimentin , an increased amount of ABC, and higher translocation of β-catenin to the nucleus in cells in cell lines transfected with the miR-92a-3p mimic, while we expected to observe decreased expression of E-Cadherin, supporting the hypothesis that this microRNA activates the EMT program. On the other hand, we expected to observe a decrease in the levels of expression of EMT-TFs, N-Cadherin, and Vimentin cell lines transfected with the miR-92a-3p inhibitor, while the expression of E-cadherin remains unaltered.

Research objective 2: Expression of *DPYD*, *TYMS*, *MTHFR*, *ERCC1*, *ERCC2*, and *XRCC1* in response to miR-92a-3p

To study the upregulation of *DPYD*, *TYMS*, *MTHFR*, *ERCC1*, *ERCC2*, and *XRCC1* expression mediated by miR-92a-3p, we analyzed SW480 and SW620 cell lines transfected with miR-92a-3p-mimic or miR-92a-3p-inhibitor. The levels of *DPYD*, *TYMS*, *MTHFR*, *ERCC1*, *ERCC2*, and *XRCC1* mRNAs were measured in SW480 and SW620 cells transfected with miR-92a-3p mimic and inhibitors by RT-qPCR. Primer sequences are specified in Appendix 1. Additionally, protein quantification by Western blot was performed for the genes that were up or downregulated in any of the transfection conditions. Antibodies used for western blot are specified in Appendix 2.

In these experiments, we expected to observe upregulation of expression of *DPYD*, *TYMS*, *MTHFR*, *ERCC1*, *ERCC2*, and *XRCC1* in response to miR-92a-3p mimic, while we expected to observe downregulation of expression in response to miR-92a-3p inhibitors, confirming that these genes are upregulated via β-catenin activation.

Research objective 3: Chemosensitivity to 5-fluorouracil-based treatments in response to miR-92a-3p

To determine the role of miR-92a-3p and the genes upregulated in the experiments previously performed on the resistance of cell lines to chemotherapeutic agents we seeded 5,000 cells per well in 96 well plates until 60% confluence. Then, different concentrations of 5-FU / L-OHP (0 μM, 25/5 μM, 50/10 μM, 75/15 μM, 100/20 μM, 150/30 μM, 200/40 μM, and 250/50 μM) were added to the culture medium of SW480 and SW620 cell lines previously transfected with miR-92a-3p mimics, inhibitors, or untreated in culture medium during 24 h. The viability of cell lines was measured after 24 h of treatment by MTT assay.

In these experiments, we expected to find that cell lines transfected with miR-92a-3p mimic oligonucleotide display decreased chemosensitivity to 5-FU / L-OHP, and the opposite for cell lines treated with the miR-92a-3p inhibitor, indicating that this microRNA is a biomarker of *in vitro* chemoresistance.

Statistical and image analysis

Results were presented as mean ± SEM. To evaluate significance of difference between samples, collected data was analyzed with GraphPad 8.0 software using an unpaired one tailed Mann-Whitney U test or two-way ANOVA. A p-value equal or less than 0.05 was considered statistically significant. Presented data is representative of three independent experiments to ensure that the obtained results are reproducible. Images were analyzed using the software ImageJ Ver.2.3.0/1.53q.

Research settings

Experiments were performed in the Laboratory of Cellular and Molecular Oncology at the Faculty of Medicine of the University of Chile.

Research funding

This research project was funded by the National Agency of Research and Development (ANID, Chile) Scholarship No. 21180195 (P.E) and partially by the Grant FONDECYT #1211948 and the Grant CYTED-P218RT0120.

RESULTS

Research objective 1: Effect of miR-92a-3p on activation of β-catenin and EMT *in vitro*

First, we tested the concentration of miR-92a-3p mimic required for transfection of each cell line. We transfected 50,000 SW480 or SW620 cells with increasing concentrations of miR-92a-3p mimic or negative control for 24 h (1 nM, 5 nM, 10 nM, 20 nM) using Lipofectamine 2000 1µL/mL in 12 well plates, then extracted miRNA from the transfected cells and quantified the relative level of miR-92a-3p through TaqMan™ RT-qPCR (**Figure 1-A**). On parallel, we transfected the cell lines with 100 nM of miR-92a-3p inhibitor or negative control, increasing the amount of Lipofectamine 2000™ reagent used in this case (2µL, 2.5µL, and 3µL), followed by miR-92a-3p quantification through TaqMan™ RT-qPCR (**Figure 1-B**).

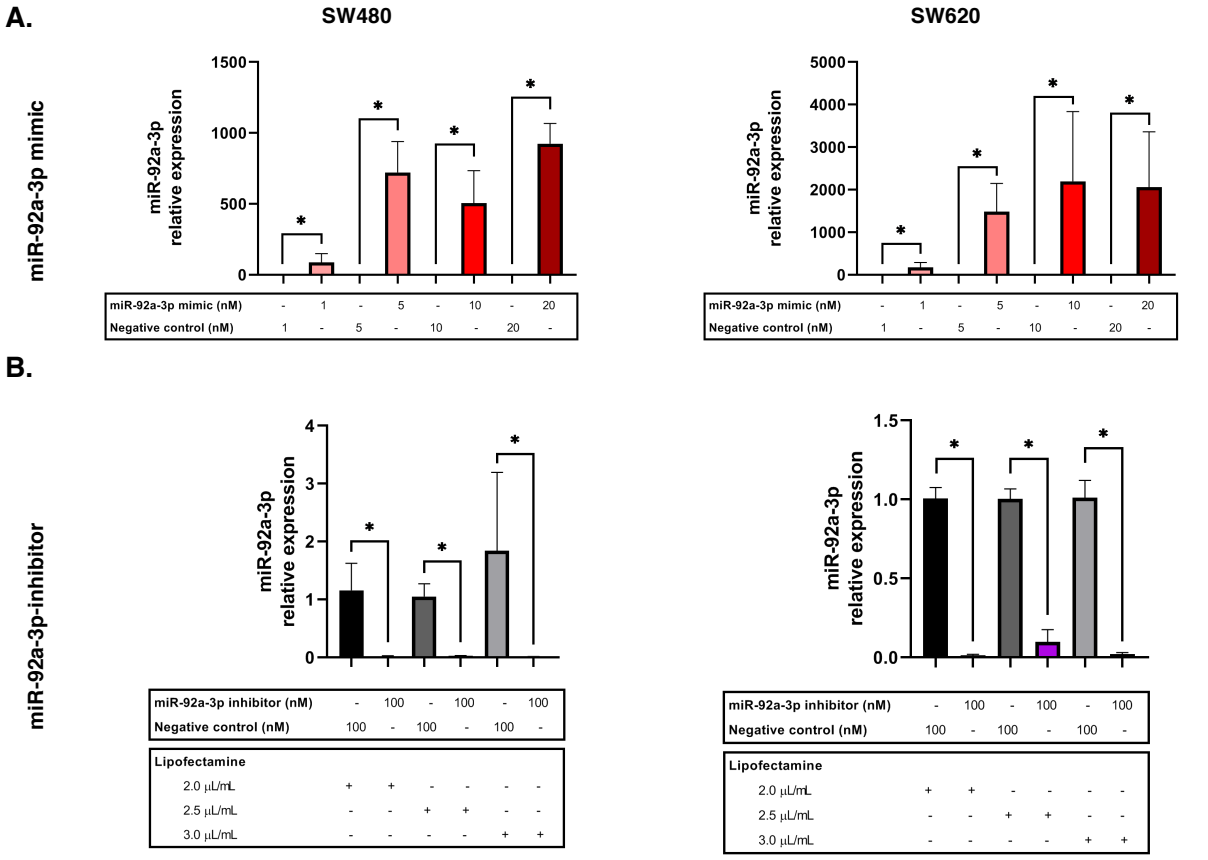

Figure 4. Transfection efficiency curve in SW480 and SW620 cell lines transfected with miR-92a-3p mimic and inhibitor oligonucleotides: **(A)** RT-qPCR analysis showing the relative expression of miR-92a-3p in SW480 and SW620 cells transfected with increasing concentrations of mimic or negative control. **(B)** RT-qPCR analysis showing the relative expression of miR-92a-3p in SW480 and SW620 cells transfected with 100 nM of inhibitor or negative control and increasing amounts of Lipofectamine 2000™ reagent. Statistical differences in miR levels were determined using the Mann-Whitney U test (*p=0.05). Data represent the means ± SEM from three independent experiments.

Based on these results, we decided that the concentration of miR-92a-3p mimic required for transfection SW480 cells is 20 nM, and 10 nM for SW620 cells. The concentration of miR-92a-3p inhibitor required for transfection of both cell lines is 100 nM with 2µL/mL of Lipofectamine 2000™ reagent.

Once the optimal concentrations of miR-92a-3p-mimic and inhibitor required for transfection were established, the expression of EMT-transcription factors *SNAIL*, *SLUG*, *ZEB1* **(Figure 5-A)**, as well as the epithelial marker E-cadherin, β-catenin, and the mesenchymal marker vimentin **(Figure 5-B)** were measured in SW480, and SW620 transfected with miR-92a-3p-mimic, miR-92a-3p-inhibitors, or control oligonucleotides by RT-qPCR.

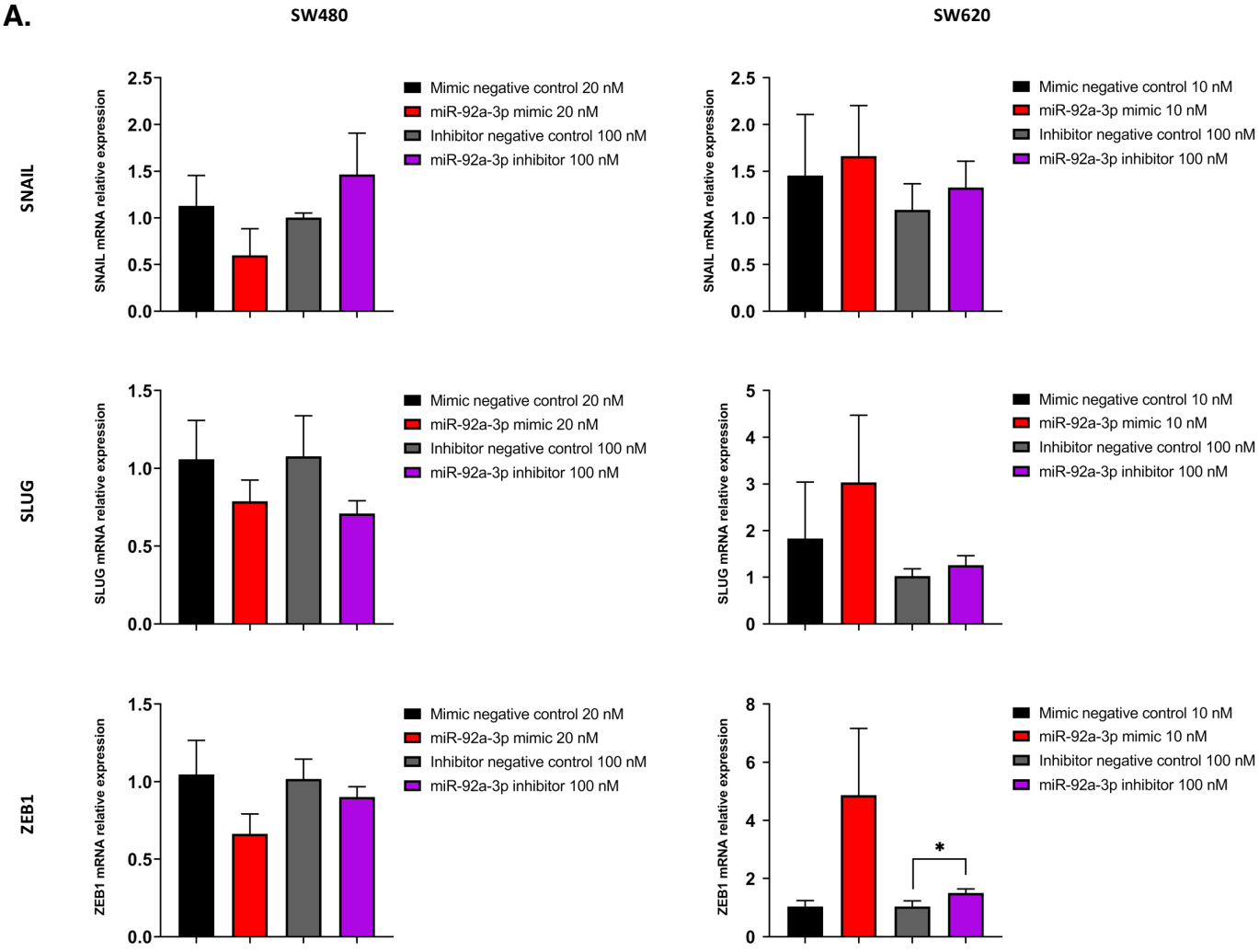

Figure 5-A. Expression of EMT-Transcription factors in SW480 and SW620 cell lines transfected with miR-92a-3p-mimic or inhibitors: RT-qPCR analysis showing the relative expression of *SNAIL*, *SLUG* and *ZEB1* upon miR-92a-3p mimic or inhibitor transfection in SW480 and SW620 cells. Statistical differences in mRNA levels were determined using the Mann-Whitney U test (*p=0.05). Data represent the means ± SEM from three independent experiments.

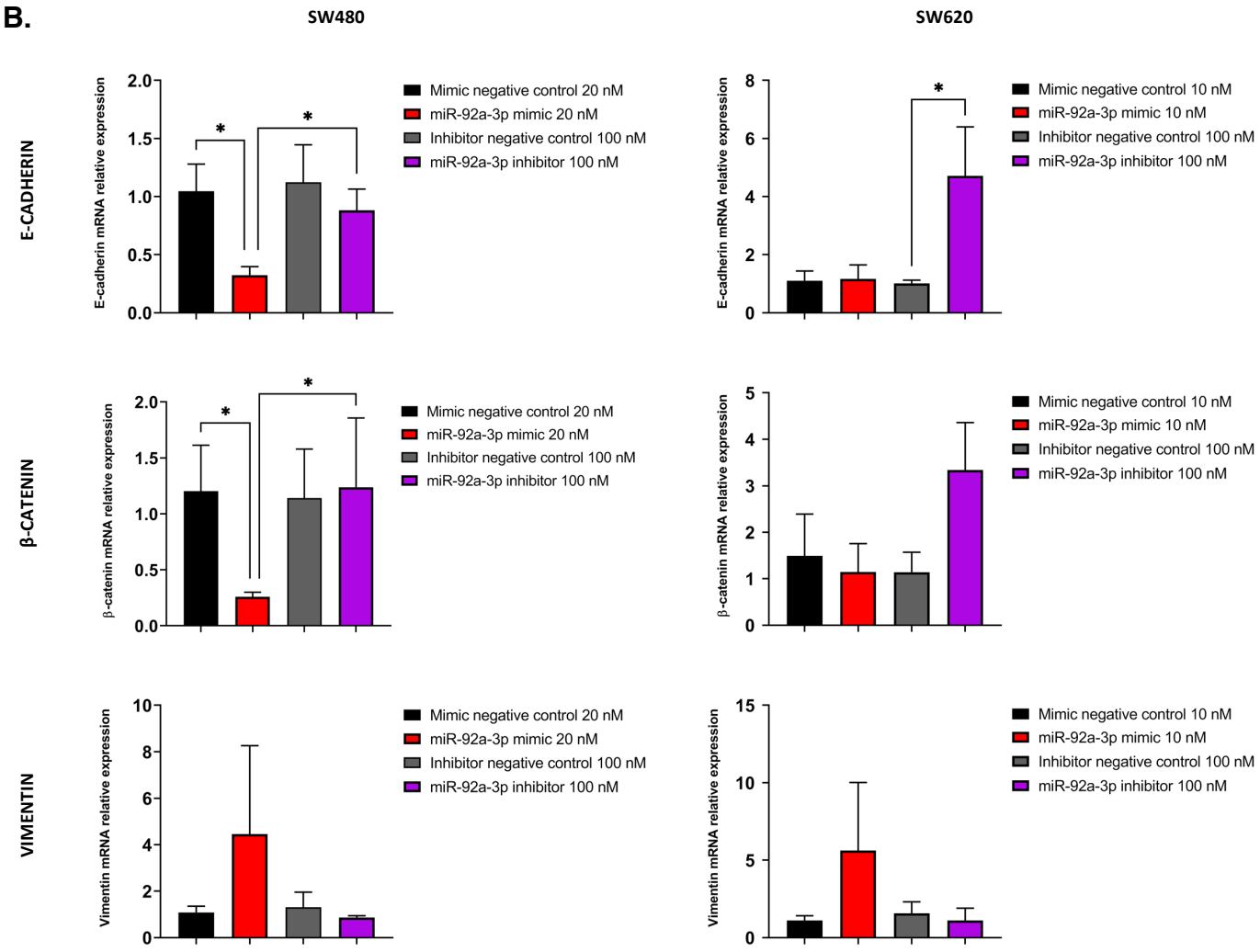

Figure 5-B. Expression of EMT markers in SW480 and SW620 cell lines transfected with miR-92a-3p-mimic or inhibitors: RT-qPCR analysis showing the relative expression of E-Cadherin, β-catenin, and Vimentin mRNA upon miR-92a-3p mimic or inhibitor transfection in SW480 and SW620 cells. Statistical differences in mRNA levels were determined using the Mann-Whitney U test (*p=0.05). Data represent the means ± SEM from three independent experiments.

Modifications in the statistical test, using a one-way Mann-Whitney U test instead of a two-way test, as we did for the analysis of transfection data, helped us better determine statistical differences in the medians of mRNA levels in treated versus untreated cells, as previously described[59]. Expression of *TWIST1* and N-Cadherin was non-detectable in the cell lines mRNA under all conditions.

We found that the expression of E-cadherin mRNA was significantly increased in the SW480 and SW620 cell lines treated with miR-92a-3p-inhibitor (p=0.05) compared to cell lines

treated with the respective negative control oligonucleotide (Fig. 5-B). We also found that the level of β-catenin mRNA was decreased in SW480 cell lines treated with miR-92a-3p-mimic, compared with the β-catenin mRNA expression for cell lines treated with the miR-92a-3p-inhibitor, and the respective mimic negative control ($p=0.05$) (Fig. 5-B). We finally found that the levels of *ZEB1* mRNA were significantly increased in SW620 cells treated with miR-92a-3p-inhibitor, although the gain was discrete ($p=0.05$) (Fig. 5-A).

Although we observed some slight differences in mRNA expression of *SNAIL*, *SLUG*, and Vimentin in SW480 and SW620 cells treated with miR-92a-3p-mimic or inhibitor compared to their respective controls, these changes were not statistically significant at mRNA level ($p>0.05$, Fig. 5-A).

We assessed whether the observed changes in mRNA expression were being inhibited by serum deprivation during the transfection by repeating the transfection of SW480 and SW620 cell lines in two additional experimental settings: transfection with miR-92a-3p-mimic using Opti-MEM™, and direct supplementation with 5% FBS 5 hours after transfection, followed by extraction of mRNA 24 hours after transfection; or in parallel, transfection of miR-92a-3p-mimic using Opti-MEM™, and change of culture medium to Leibovitz's L-15 supplemented with 10% FBS, followed by extraction of mRNA 24 hours after transfection. In both experimental conditions with serum supplementation, the increase of miR-92a-3p-mimic was significantly impaired by the addition of FBS (Appendix 3). Moreover, although changes in the mRNA levels of some of the genes of interest were observed, we found that the biomarker of epithelial phenotype, E-cadherin, was not significantly downregulated in SW480 cells, indicating failure to achieve EMT in these modified experimental settings. Although we observed downregulation of E-cadherin expression in SW620 cells ($p=0.05$), these changes were not enough to imply any benefit in transfection by the addition of FBS (Appendix 4). Therefore, we performed the rest of the experiments using unsupplemented Opti-MEM™ during the transfection process, according to the instructions from the manufacturer.

Following our findings, we decided to determine if the observed changes in expression of E-cadherin and β-catenin mRNA correlated with changes in protein expression. SW480 and SW620 cell lines were transfected with miR-92a-3p-mimic, inhibitor, or negative control oligonucleotides, maintaining the original experimental conditions (unsupplemented Opti-MEM™) for 24 hours, followed by protein extraction and protein expression analysis of E-cadherin and β-catenin. We also assessed the levels of ABC with specific antibodies. Western blot images and protein quantification relative to β-actin are shown in **Figure 6.**

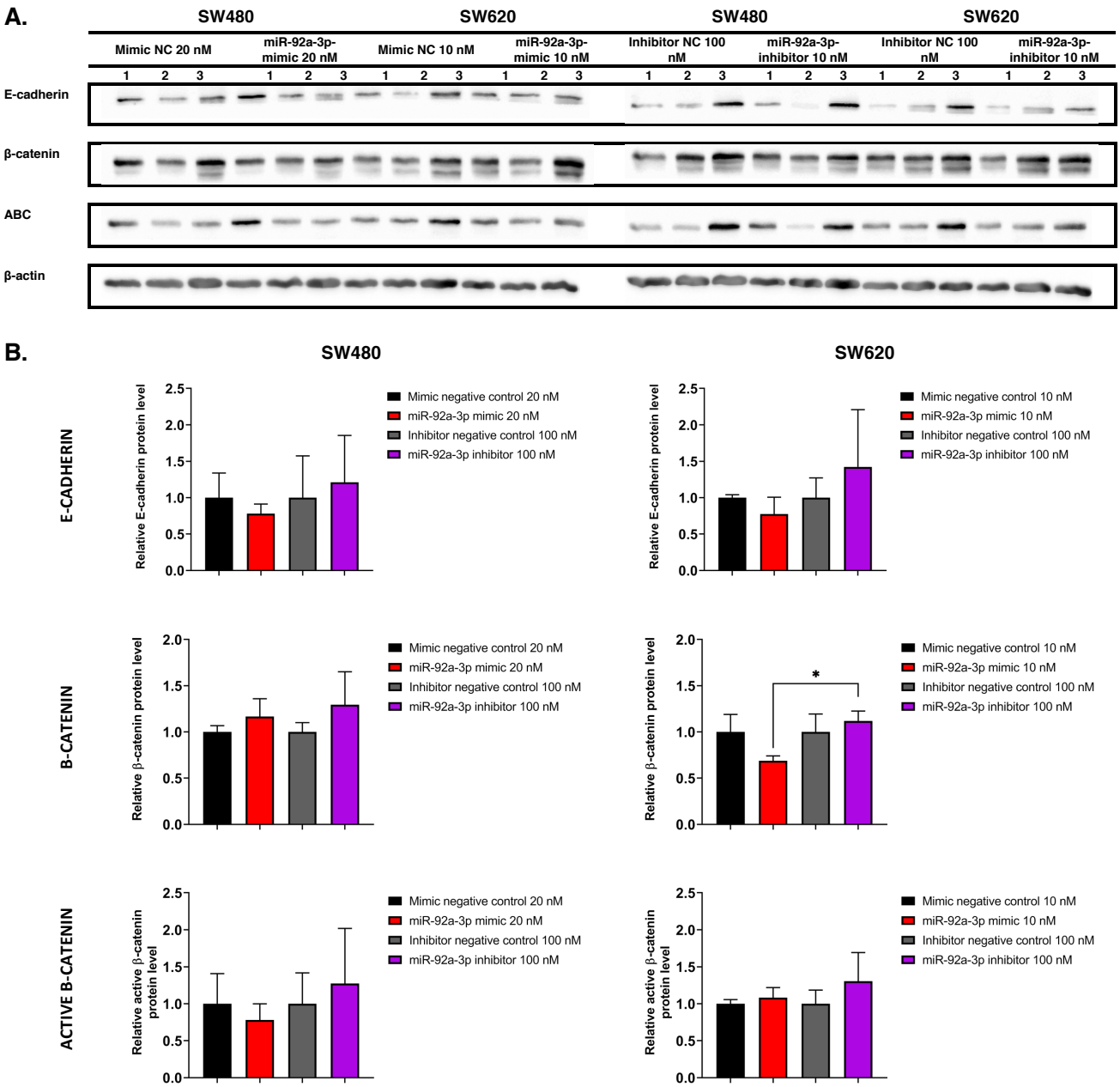

Figure 6. Protein expression of EMT-Transcription factors and EMT markers in SW480 and SW620 cell lines transfected with miR-92a-3p-mimic or inhibitors: **(A)** Western blot analysis showing the proteins levels of E-Cadherin, β-catenin, active β-catenin (ABC), and β-actin upon miR-92a-3p mimic or inhibitor transfection in SW480 and SW620 cells. **(B)** Quantification of E-Cadherin, β-catenin, and ABC proteins levels relative to β-actin upon transfection with miR-92a-3p mimic or inhibitor in SW480 and SW620 cells. Statistical differences in mRNA levels were determined using the Mann-Whitney U test (*p=0.05). Data represent the means ± SEM from three independent experiments.

In this experiment, we observe that E-cadherin and ABC protein levels are not affected by transfection with miR-92a-3p-mimic or inhibitor. We only observe a significant difference in β-catenin protein levels between SW620 cells transfected with miR-92a-3p-mimic versus miR-

92a-3p-inhibitor (p=0.05). However, we did not find a significant difference in β-catenin protein level between SW620 cells transfected with mimic, inhibitor, and their respective experimental negative controls. These results suggest that changes in miR-92a-3p levels are not enough to modify the expression of E-cadherin, β-catenin, and ABC protein levels in our chosen experimental conditions (Fig. 6-B).

To further elucidate if miR-92a-3p has a role in promoting the activation of β-catenin, we assessed β-catenin subcellular localization in SW480 and SW620 cells transfected with miR-92a-3p mimic or inhibitor for 24 hours by immunofluorescence confocal microscopy. In parallel, we treated SW480 and SW620 cell lines with SB-216763 10 μM to activate the Wnt/β-catenin pathway, or with IWR-1-endo 10 μM to inhibit Wnt/β-catenin signaling for 24 hours, followed by immunofluorescence analysis. Because both SB-216763 and IWR-1-endo were solubilized in DMSO, cell lines were treated with an equivalent concentration of solvent (DMSO 0.81 μL/1 mL Opti-MEM™) for 24 h and analyzed by immunofluorescence afterward as an additional control. Further controls include untreated SW480 and SW620 cells maintained in unsupplemented Opti-MEM™, and Leibovitz´s L15 + 10% SFB. The results of transfection with miR-92a-3p mimic or inhibitor, their respective negative control oligonucleotides, and untreated cells in Opti-MEM™ are shown in **Figures 7-A and 7-B.** Colocalization images were obtained using the Colocalization Threshold tool in ImageJ. Immunofluorescence confocal microscopy images with 40X objective of SW480 and SW620 cells treated with IWR-1-endo 10 μM, SB-216763 10 μM, DMSO 0.81 μL/mL, and Leibovitz´s L15 + 10% FBS are shown in Appendix 5 and 6. Additionally, confocal microscopy images with 10X magnification for all experimental conditions can be found in Appendix 7 (SW480) and 8 (SW620).

DMSO is the recommended vehicle for IWR-1-endo and SB-216763 stock solution preparation because of the low solubility and instability of these molecules in an aqueous solution. Unfortunately, it was extremely toxic for both SW480 and SW620 cells, evidenced by the loss of normal cell morphology and cell shrinkage in all cell lines treated with DMSO (Appendix 5-6). In addition, we observed an unspecific signal in the extracellular field of SW480 and SW620 cells treated with SB-216763 in the green channel, which made the images unusable for our analysis. We decided that both IWR-1-endo and SB-216763 were unsuitable as positive and negative controls for our experimental design, a problem that we propose could have been avoided by working with more concentrated stock solutions (0,5 mg/mL, equivalent to IWR-1-endo 1.24 μM and SB-216763 1.35 μM). Therefore, we decided to continue our experiments only with mimic and inhibitor transfection.

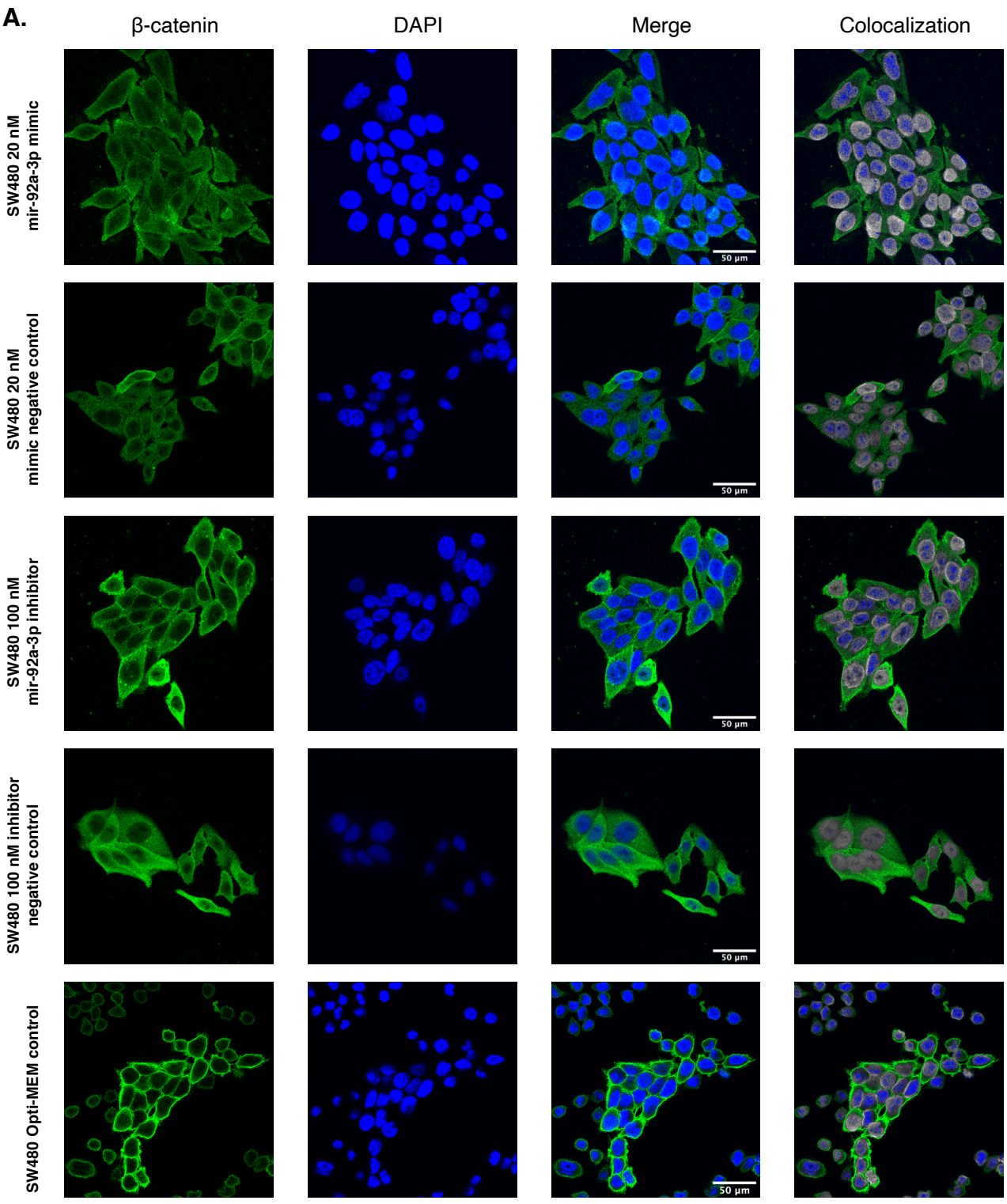

Figure 7-A: Expression and β-catenin subcellular localization in response to miR-92a-3p in SW480 and SW620 cells (40X magnification): 20.000 SW480 cells per well were seeded and transfected after 65 hours with miR-92a-3p mimic, miR-92a-3p inhibitor, or their corresponding negative controls for 24 hours, then fixed and examined by immunofluorescence for β-catenin (green), and DAPI (blue) for the nuclei as reference. Colocalization images were constructed using the Colocalization Threshold tool, indicating areas of green and blue fluorescence signal overlapping (grey).

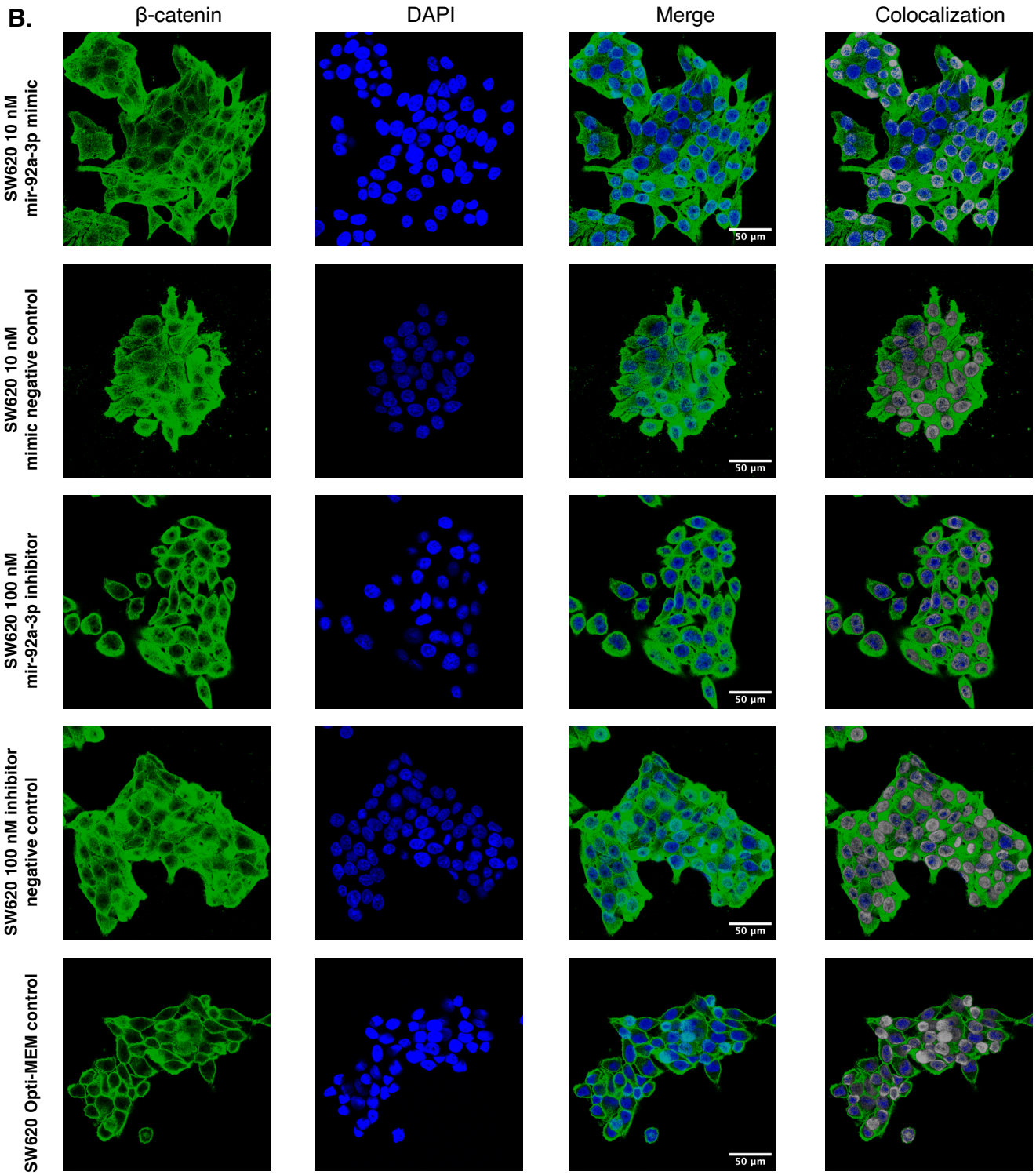

Figure 7-B: Expression and β-catenin subcellular localization in response to miR-92a-3p in SW480 and SW620 cells (40X magnification): 20.000 SW620 cells per well were seeded and transfected after 65 hours with miR-92a-3p mimic, miR-92a-3p inhibitor, or their corresponding negative controls for 24 hours, then fixed and examined by immunofluorescence for β-catenin (green), and DAPI (blue) for the nuclei as reference. Colocalization images were constructed using the Colocalization Threshold tool, indicating areas of green and blue fluorescence signal overlapping (grey).

In the presented images, we observe membrane localization of β-catenin in both untreated SW480 and SW620 cell lines in Opti-MEM™ culture medium, with low cytosolic green fluorescence and a small proportion of cells displaying nuclear localization of β-catenin in SW620 cells. On the contrary, we observe a change in β-catenin fluorescence localization in SW480 and SW620 cells transfected with miR-92a-3p mimic, miR-92a-3p inhibitor, and their corresponding negative controls, indicating that β-catenin distribution is mostly being affected by the transfection process rather than by changes in miR-92a-3p levels. In transfected cells, green fluorescence is localized predominantly in the cell cytosol and, to a lesser extent, in the cell nucleus. We also observe a significant cell enlargement. Indeed, colocalization analysis shows a higher overlap of green and blue fluorescence in transfected cells, particularly in cells transfected with the mimic and inhibitor negative controls, which is opposite to our predictions (Fig. 7-A, 7-B).

Confocal microscopy images at 10X magnification provide us further evidence that changes in β-catenin fluorescence intensity are not being mediated by miR-92a-3p levels, as SW620 cells treated with 100 nM inhibitor negative control oligonucleotide show as much fluorescence as the ones untreated (Opti-MEM control), and both show higher fluorescence compared with the images from SW620 cells transfected with 10 nM mimic negative control oligonucleotide, even though all photos correspond to negative controls and therefore, should only display baseline levels of β-catenin fluorescence (Appendix 8). Confocal 10X magnification images from SW480 cells seem to show results better aligned with what we expected to find according to our hypothesis, although the differences are not enough to establish a clear tendency (Appendix 7).

To further assess potential differences in β-catenin fluorescence intensity in our images, we performed a semiquantitative analysis of β-catenin mean fluorescence, integrated density and colocalization of green and blue fluorescence (Appendix 9).

Our results corroborate the previous western blot result (Fig. 6-B), in which increased levels of miR-92a-3p through transfection with miR-92a-3p mimic did not correlate with decreased β-catenin protein levels in SW480 or SW620 cells compared with negative control transfection, and the treatment with miR-92a-3p inhibitor also failed to exert any effect in β-catenin protein expression (Appendix 9-A, 9-B).

Images obtained with 40X objective were processed with the ImageJ JACoP™ tool to establish colocalization of β-catenin (green fluorescence) and DAPI (blue fluorescence), which would indicate translocation of β-catenin into the nucleus. According to our hypothesis, we

expected to find higher overlapping and Pearson's coefficients for SW480 and SW620 cells treated with miR-92a-3p mimic, and lower coefficients for cells treated with miR-92a-3p inhibitor. Unfortunately, our results did not provide evidence of β-catenin nuclear translocation associated with miR-92a-3p levels (Appendix 9-C, 9-D).

Based on our current results, we decided not to continue with further migration and invasion assays, as our experiments provide clear evidence that transient changes in miR-92a-3p levels achieved through mimic or inhibitor transfection fail to induce significant EMT in SW480 and SW620 cells in our experimental settings.

Research objective 2: Expression of *DPYD*, *TYMS*, *MTHFR*, *ERCC1*, *ERCC2*, and *XRCC1* in response to miR-92a-3p

We analyzed the data of mRNA expression from SW480 and SW620 cell lines transfected with miR-92a-3p-mimic, miR-92a-3p-inhibitor, or negative controls for expression of *DPYD*, *TYMS*, *MTHFR*, *ERCC1*, *ERCC2*, and *XRCC1* by RT-qPCR using the one tail the Mann-Whitney U test. The results are shown in **Figures 8-A** and **8-B.**

A.

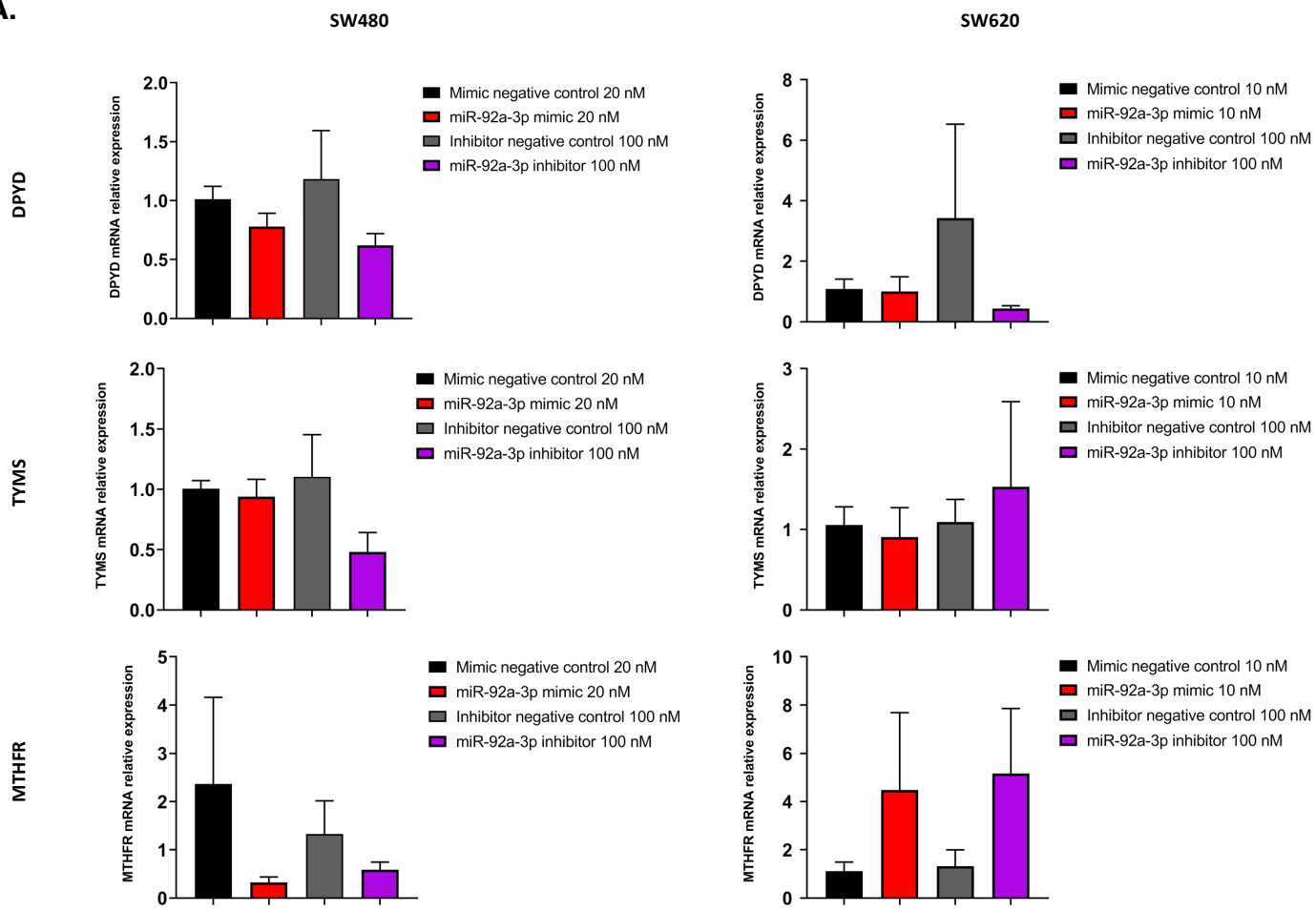

Figure 8-A. Expression of genes associated with 5-FU response in SW480 and SW620 cell lines transfected with miR-92a-3p-mimic or inhibitors: RT-qPCR analysis showing the relative expression of *DPYD*, *TYMS* and *MTHFR* mRNA upon miR-92a-3p mimic or inhibitor transfection in SW480 and SW620 cells. Statistical differences in mRNA levels were determined using the Mann-Whitney U test (*p=0.05). Data represent the means ± SEM from three independent experiments.

B.

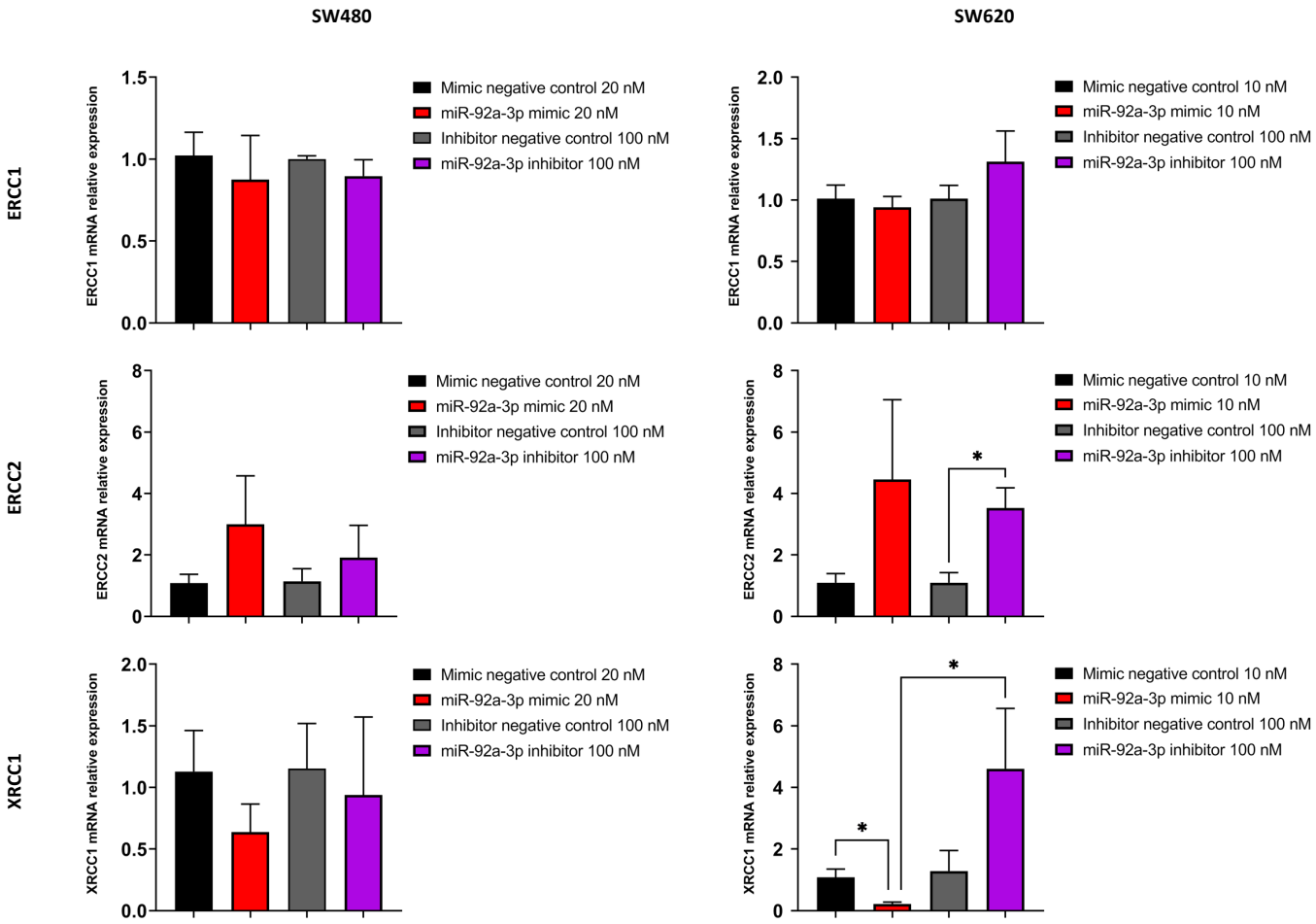

Figure 8-B. Expression of genes associated with L-OHP response in SW480 and SW620 cell lines transfected with miR-92a-3p-mimic or inhibitors: RT-qPCR analysis showing the relative expression of *ERCC1*, *ERCC2*, and *XRCC1* mRNA upon miR-92a-3p mimic or inhibitor transfection in SW480 and SW620 cells. Statistical differences in mRNA levels were determined using the Mann-Whitney U test (*p=0.05). Data represent the means ± SEM from three independent experiments.

In this experiment, we observed a significant increase in *ERCC2* mRNA levels in SW620 cells treated with miR-92a-3p inhibitor compared with cells transfected with negative control (p=0.05). We also find a significant decrease in *XRCC1* mRNA levels in SW620 cells transfected with miR-92a-3p-mimic compared to its negative control (p=0.05) and with cells transfected with miR-92a-3p-inhibitor (p=0.05). Analysis of SW480 and SW620 cells treated with IWR-1-endo and SB-216763 was not performed because of the effect of DMSO on cell viability (Appendix 5 and 6).

As in the previous research objective, we assessed whether the observed changes in mRNA expression were being inhibited by serum deprivation by repeating the transfection experiments with miR-92a-3p-mimic using supplemented Opti-MEM™ + 5% FBS and Leibovitz's L-15 + 10% FBS. The results displayed in Appendix 10 show that except for an increase in *XRCC1* mRNA expression in SW480 cells treated with Opti-MEM™ + 5% FBS (p=0.05), changes in mRNA levels of *DPYD*, *TYMS*, *MTHFR*, *ERCC1*, *ERCC2*, and *XRCC1* in transfected SW480 and SW620 cells were not impaired by serum deprivation.

Continuing with our experiments, we assessed whether the changes observed in *ERCC2* and *XRCC1* mRNA levels are reflected at the protein level. We transfected SW480 and SW620 cell lines with miR-92a-3p-mimic, miR-92a-3p-inhibitor, or negative controls for 24 hours, followed by protein extraction and protein expression analysis of *ERCC2* and *XRCC1*. The results of our experiments are shown in **Figure 9.**

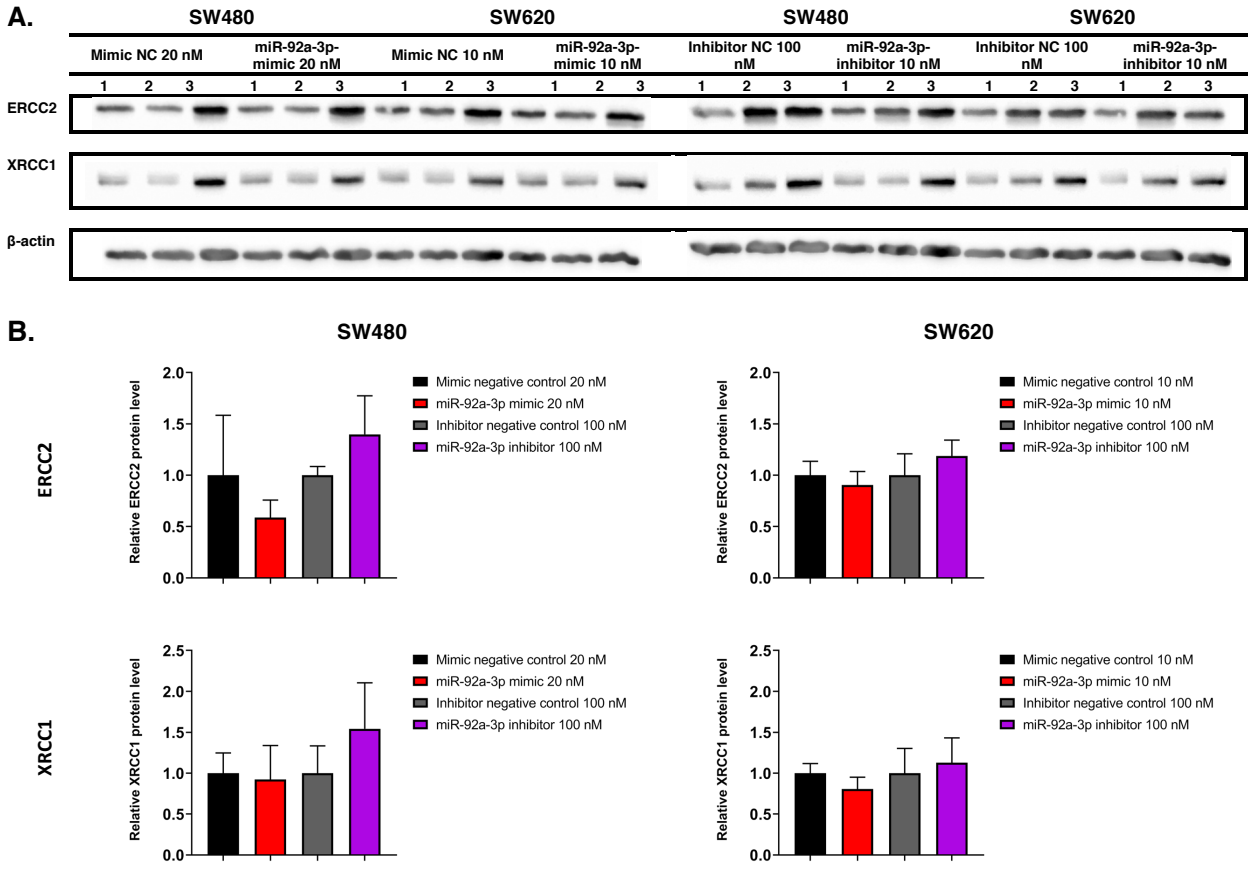

Figure 9. Protein expression of genes associated with 5-FU and L-OHP in SW480 and SW620 cell lines transfected with miR-92a-3p-mimic or inhibitors: **(A)** Western blot analysis showing the proteins levels of E-Cadherin, β-catenin, ABC, and β-actin upon miR-92a-3p mimic or inhibitor transfection in SW480 and SW620 cells. **(B)** Quantification of E-Cadherin, β-catenin, and ABC proteins levels relative to β-actin upon transfection with miR-92a-3p mimic or inhibitor in SW480 and SW620 cells. Statistical differences in mRNA levels were determined using the Mann-Whitney U test (*p=0.05). Data represent the means ± SEM from three independent experiments.

Western blot results showed that *ERCC2* and *XRCC1* protein levels in SW480 and SW620 were not significantly different in SW480 and SW620 transfected with miR-92a-3p-mimic or inhibitor compared with control oligonucleotides (Fig. 9-B). Overall, the results of these experiments show that changes in miR-92a-3p levels did not exert effects on protein levels *DPYD*, *TYMS*, *MTHFR*, *ERCC1*, *ERCC2*, and *XRCC1* in SW480 and SW620 cell lines in our experimental model.

Research objective 3: Chemosensitivity to 5-fluorouracil-based treatments in response to miR-92a-3p

We transfected 5,000 SW480 and SW620 cells with miR-92a-3p-mimic, miR-92a-3p-inhibitor, negative controls, or Opti-MEM™ as untreated control. One hour after transfection, the cells were treated with increasing concentrations of 5-FU / L-OHP for 24 hours, then viability of cell lines was measured through MTT assay. The results of the experiments are shown in **Figure 10** and **Table 1**.

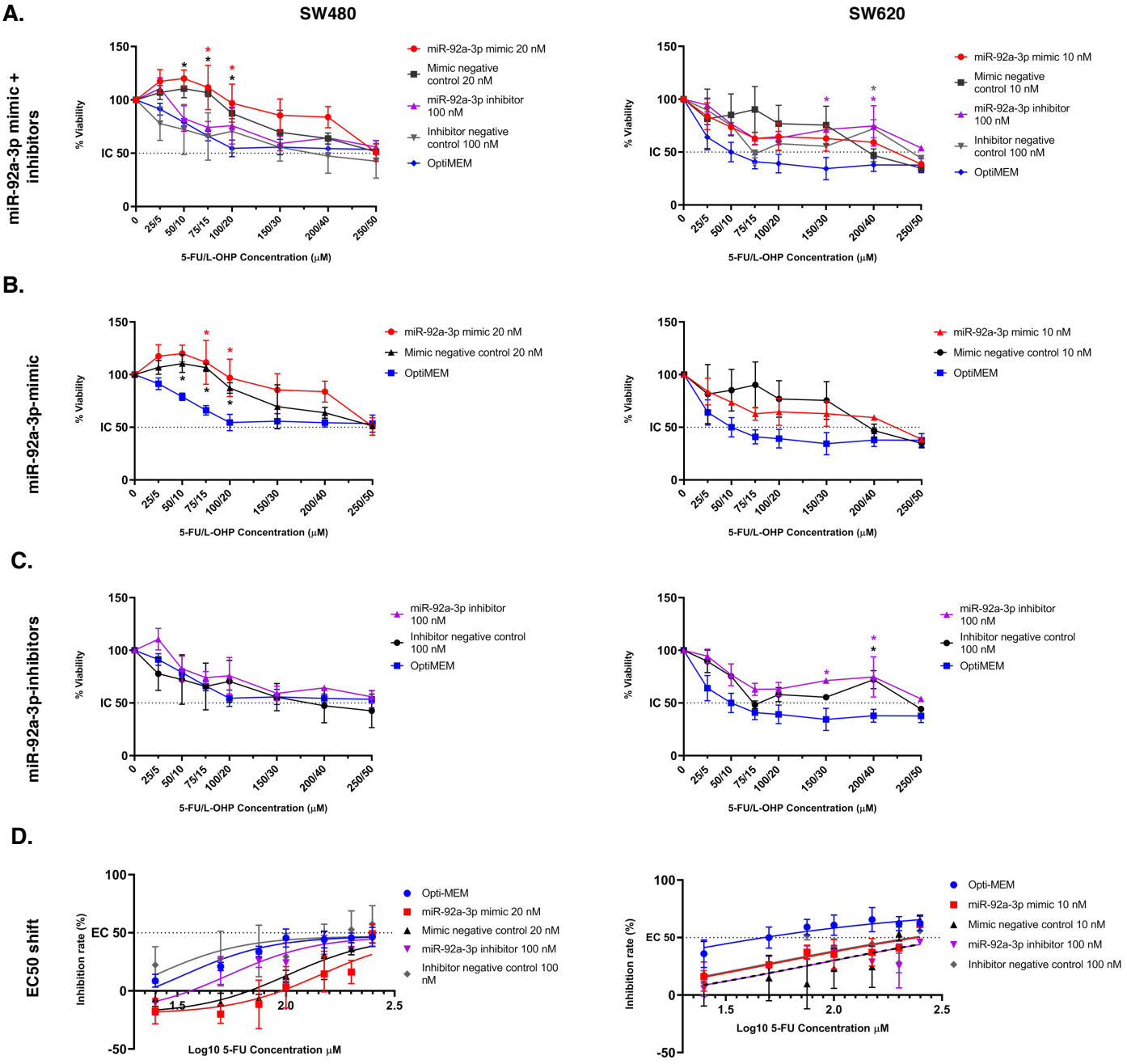

Figure 10: Dose-response curve for SW480 and SW620 cells treated with 5-FU / L-OHP: SW480 and SW620 cells were seeded in a 96 well plate (5,000 cells/plate) and transfected with miR-92a-3p-mimic (**A,B**), miR-92a-3p-inhibitors (**A,C**), negative controls, or Opti-MEM™ and one hour after transfection were treated with increasing concentrations of 5-FU / L-OHP (0 µM, 25/5 µM, 50/10 µM, 75/15 µM, 100/20 µM, 150/30 µM, 200/40 µM, and 250/50 µM) during 24 h**. D:** Inhibition-response curve and best-fit response models for each treatment. The viability of cell lines was then measured by MTT assay. Statistical differences were determined using Two-way ANOVA test and non-linear regression (*p<0.05). Data represent the means ± SEM from three independent experiments.

Table 1: IC50 for cells treated with miR-92a-3p-mimic, miR-92a-3p-inhibitors, negative controls, or untreated.

	IC50 5-FU/ L-OHP (µM)	**95% CI 5-FU / L-OHP (µM)**	**R^2**	***P***
SW480				
Opti-MEM (untreated)	193.5 / 38.71	154.9 to 244.2 / 30.98 to 48.83	0.7203	Ref.
miR-92a-3p mimic 20 nM	842.1 / 168.42	398.2 to 4319 / 79.65 to 863.8	0.2204	<0.0001*
Mimic negative control 20 nM	465.0 / 93.0	299.7 to 814.4 / 59.94 to 162.9	0.4873	<0.0001*
miR-92a-3p inhibitor 100 nM	297.7 / 59.53	210.5 to 440.4 / 42.10 to 88.09	0.5464	0.0331*
Inhibitor negative control 100 nM	172.6 / 34.51	101.3 to 307.0 / 20.26 to 61.40	0.3045	0.6577
SW620				
Opti-MEM (untreated)	68.35 / 13.67	48.74 to 94.66 / 9.748 to 18.93	0.6246	Ref.
miR-92a-3p mimic 10 nM	188.8 / 37.77	142.2 to 254.3 / 28.45 to 50.86	0.5987	0.0001*
Mimic negative control 10 nM	250.0 / 50.01	143.7 to 479.4 / 28.74 to 95.89	0.3266	0.0014*
miR-92a-3p inhibitor 100 nM	281.2 / 56.23	194.0 to 427.0 / 38.81 to 85.40	0.3401	<0.0001*
Inhibitor negative control 100 nM	183.7 / 36.74	133.1 to 258.2 / 26.62 to 51.65	0.489	<0.0001*

IC: inhibitory concentration of 5-FU / L-OHP required to decrease viability of each cell line by 50%. CI: confidence interval. Ref: Reference value.

The results of these experiments show that the baseline inhibitory concentration of 5-FU / L-OHP required to decrease viability of each cell line by 50% (IC50) is 193.5 / 38.71 µM for SW480 cells (CI 95%: 154.9 / 30.98 µM to 244.2 / 48.83 µM), and 68.35 / 13.67 µM for SW620 cells (CI 95%: 48.74 / 9.748 µM – 94.66 / 18.93 µM) at 24 hours of treatment (Table 1).

Transfection with miR-92a-3p-mimic increased IC50 to 842.1 / 168.42 µM (CI 95%: 398.2 / 79.6 µM to 4319 / 863.8 µM, p<0.0001), although transfection with negative control also increased the IC50 to 465.0 / 93.0 µM (CI 95%: 299.7 / 59.9 µM to 814.4 / 162.9 µM, p<0.0001). In the same experiment with SW620 cells we observe that the IC50 is increased in a statistically significant manner for cells transfected with miR-92a-3p-mimic (IC50 188.8 / 37.77 µM, CI 95%: 142.2 / 28.45 µM to 254.3 / 50.86 µM, p=0.0001), and is even higher for cells transfected with

negative control (IC50 250.0 / 50.01 μM, CI 95%: 143.7 / 28.74 μM to 479.4 / 95.89 μM, p=0.0014) (Table 1).

Two-way ANOVA analysis for each concentration showed that viability of SW480 cells increased with miR-92a-3p-mimic transfection at 75/15 μM (viability untreated: 66.11%, transfected 111.6%, p=0.0234), and 100/20 μM (viability untreated: 54.52%, transfected 96.89%, p=0.0411), while mimic negative control treatment increased viability at 50/10 μM (viability untreated: 78.91%, transfected 110.5%, p=0.0384), 75/15 μM (viability untreated: 66.11%, transfected 106.6%, p=0.0039), and 100/20 μM (viability untreated: 54.52%, transfected 87.27%, p=0.0287). No statistically significant differences in viability were observed at any other concentration between SW480 cells treated with miR-92a-3p-mimic and negative control, or at any specific 5-FU / L-OHP concentration between SW620 cells treated with miR-92a-3p-mimic, negative control, and untreated cells (Fig. 10-B).

SW480 cells transfected with miR-92a-3p-inhibitor show an increased IC50 (297.7 / 59.53 μM, CI 95%: 210.5 / 42.10 μM to 440.4 / 88.09 μM, p=0.0331), while transfection with inhibitor negative control show similar results as untreated cells (IC50 172.6 / 34.51 μM, CI 95%: 101.3 / 20.26 μM to 307.0 / 61.40 μM, p=0.6577) (Table 1). Two-way ANOVA analysis shows no difference at any specific concentration between SW480 cells treated with miR-92a-3p-inhibitor, negative control, or untreated cells (Fig. 10-C).

Transfection of SW620 cells show that treatment with inhibitor negative control increases IC50 compared to untreated cells (IC50 183.7 / 36.74 μM, CI 95%: 133.1 / 26.62 μM to 258.2 / 51.65 μM, p<0.0001), as well transfection with miR-92a-3p-inhibitor (IC50 281.2 / 56.23 μM, CI 95%: 194.0 / 38.81 μM to 427.0 / 85.40 μM, p<0.0001) (Table 1). Two-way ANOVA analysis shows increased viability for SW620 cells transfected with miR-92a-3p-inhibitor at 150/30 μM (viability untreated: 34.39%, transfected 71.26%, p=0.0328) and 200/40 μM (viability untreated: 37.89%, transfected 74.76%, p=0.0328), while SW620 cells transfected with inhibitor negative control showed increased viability at 200/40 μM (viability untreated: 37.89%, transfected 72.1%, p= 0.0328) (Fig. 10-C).

Nonlinear regression was used to determine if there is a shift in the dose-response curve (Fig. 10-D, Table 2), here expressed as the half-maximal effective concentration (EC50) ratio, indicating that a cell line is less sensible to 5-FU / L-OHP treatment (EC50 ratio>1) because of transfection, or that sensitivity to chemotherapy is increased (EC50 ratio<1). In this case, we only observed a statistically significant shift in the 5-FU / L-OHP dose-response curve for

SW480 cells transfected with miR-92a-3p-mimic (EC50 ratio: 4.122, p=0.0444), and with mimic negative control (EC50 ratio: 2.685, p=0.0026).

Table 2: EC50 shift for cells treated with miR-92a-3p-mimic, miR-92a-3p-inhibitors, negative controls, or untreated.

	EC50 ratio	**95% CI EC50 ratio**	***P***
SW480			
Opti-MEM (untreated)	Ref.	-	-
miR-92a-3p mimic 20 nM	4.122	2.516 to 7.505	0.0444*
Mimic negative control 20 nM	2.685	1.867 to 4.266	0.0026*
miR-92a-3p inhibitor 100 nM	1.649	N.C.	N.C.
Inhibitor negative control 100 nM	0.814	N.C.	N.C.
SW620			
Opti-MEM (untreated)	Ref.		-
miR-92a-3p mimic 10 nM	4.49	2.352 to 16.04	0.4503
Mimic negative control 10 nM	6.722	2.689 to N.C	0.0767
miR-92a-3p inhibitor 100 nM	10.57	N.C.	N.C.
Inhibitor negative control 100 nM	4.623	N.C.	N.C.

EC50: effective concentration of 5-FU / L-OHP required to decrease viability of each cell line by 50%. EC50 ratio: ratio of EC50 for transfected cells divided by EC50 of cells untreated. CI: confidence interval. N.C.: Non-computable. (*) Indicates a statistically significant difference (P<0.05). Ref: Reference value.

In summary, these results suggest that an increase in miR-92a-3p levels seems to affect the sensitivity of SW480 cells to 5-FU / L-OHP treatment, evidenced by a significant increase in IC50 and EC50 ratio. However, similar changes were observed for SW480 cells transfected with mimic negative control, and no statistically significant difference was found between the IC50 and EC50 ratio of SW480 cells transfected with miR-92a-3p-mimic and control (results not shown).

No significant effect on the sensitivity of SW620 cells to 5-FU / L-OHP treatment could be established, as the change in IC50 could not be confirmed by a shift in the dose-response curve. Therefore, we cannot dismiss the possibility that any observed changes may be a consequence of the transfection treatment itself rather than changes in miRNA bioavailability.

DISCUSSION

In this work, we successfully achieved a transient increase of miR-92a-3p by transfection of miR-92a-3p mimic, and a significant decrease in miR-92a-3p by transfection of miR-92a-3p inhibitor in both SW480 and SW620 cells after 24 hours. However, miR-92a-3p mimic was significantly reduced 48 hours after treatment in SW620 cells (Appendix 11), which indicates that changes in miR-92a-3p by transfection of mimics and inhibitors are not persistent for more than 24 hours.

Furthermore, the expression of EMT-TFs (*SNAIL*, *SLUG*), vimentin, as well as some genes related to chemotherapy sensitivity (*DPYD*, *TYMS*, *MTHFR*, and *ERCC1*) was not significantly affected by changes in miR-92a-3p induced by miR-92a-3-mimic or miR-92a-3p-inhibitor oligonucleotides at mRNA. However, we observed statistically significant changes in mRNA levels of E-cadherin, β-catenin, *ZEB1*, *ERCC2*, and *XRCC1*, which unfortunately did not reflect in the protein levels of these genes.

Increasing the sample size may be needed to detect changes in mRNA and protein levels in response to transfection with miR92a-3p mimic and inhibitor oligonucleotides. Although performing the experiments in triplicate may be enough to determine changes in mir-92a-3p levels in transfected cells, these may lack the statistical power for detecting less drastic changes in response to this microRNA. SW480 and SW620 cells transfected with miR-92a-3p mimic show a remarkable tendency that suggests an increase of vimentin mRNA, while SW620 cells transfected with miR92a-3p mimic show non-significant changes in expression of *SLUG* that may need to be further assessed in future experiments.

These results themselves are not enough to discard the potential influence of miR-92-a-3p on the expression of these genes in SW480 and SW620 cells, as time of transfection is an important factor that needs to be taken into consideration. Indeed, previous research regarding the role of miR-92-a-3p on chemoresistance and cancer progression used a viral miR-92-a-3p-expression vector[23] or transfection with miR-92-a-3p-mimic and inhibitor oligonucleotides that persisted in the transfected cells for 48 hours[24,25]. Some non-significant changes in protein expression of E-cadherin, ABC, *ERCC2*, and *XRCC1* could indicate some trends that would have been more notorious with a transfection strategy that lasted longer, particularly in SW480 cells in which the observed trends seem to be more remarkable.

Moreover, predesigned microRNA mimic oligonucleotides based on chemically modified double DNA strands are widely used for transient transfection of microRNAs *in vitro*. Nevertheless, transfection of high levels of these oligonucleotides (>100 nM) has shown to cause intracellular accumulation of high-weight RNA species and decreased cell viability while transfection with a lower concentration of mimics (0,5 – 1 nM) led to an increase of microRNA concentration comparable to those obtained with lentiviral transduction and plasmid transfection, but failed to suppress target gene expression compared with the later experimental strategies[60]. This indicates that the use of microRNA mimics may have a lower functional impact on cell behavior, perhaps contributing to the modest results observed in our experiments.

Nonetheless, based on the observed downregulation of E-cadherin mRNA, we can state that some degree of EMT occurred in transfected SW480 and SW620 cells. The direct target of the E-cadherin mRNA 3'-UTR by miR-92a-3p is not predicted by microRNA target prediction tools like miRDB™ or Targetscan 8.0™ but has been experimentally reported in ESCC cell lines by luciferase reporter assay[26]. Activation of EMT, downregulation of E-cadherin, and increased expression and nuclear fractions of β-catenin have also been observed in response to increased miR-92a-3p[23,25,27].

Alternatively, increased miR-92a-3p has revealed to promote migration and invasion in colorectal cancer, glioma, and ESCC cell lines by directly targeting PTEN, leading to activation of the Pi3K/Akt signaling pathway[24,27,28]. However, miR-92a-3p showed to target SOX4 in prostate cancer cell lines and downregulate Akt signaling by targeting Notch1 in glioma stem cells and Wilms tumor cells, inhibiting invasion, migration, and proliferation, showing that the response to microRNAs may be heavily influenced by the experimental model and cell type[25,61,62].

Regarding the results of the immunofluorescence assays, we observe that transfection with Lipofectamine 2000™ reactant modifies β-catenin localization in transfected cells, and contrary to our results, we even observe higher colocalization of β-catenin fluorescence in SW480 and SW620 treated with both control oligonucleotides. Although we cannot determine definitive results from our semiquantitative analysis because of sample size, we can observe a trend in transfected cells behavior compared to untreated cells and establish that the results indeed do not confirm our hypothesis.

Lipofectamine 2000™ is one of the most widely used transfection reagents, based on the formation of cationic lipid vesicles that effectively deliver DNA or RNA molecules to the

treated cells with minimal disruption of cell viability[63]. However, it has been reported that Lipofectamine 2000™ transfection exerts disturbances in the cell cycle of transfected HEK293 cells[64]. From our results, we cannot clearly state if the observed changes in β-catenin subcellular distribution and cell morphology occur due to changes in cellular behavior as consequence of the transfection process, or if it involves the direct disruption of the cell membrane integrity by incorporation of Lipofectamine liposomes, even though we used this transfection reagent within the limits of the manufacturer's suggested range. The remarkable increase in cell size of all transfected cells versus untreated may be further evidence of cell membrane disruption.

The *in vitro* chemosensitivity analysis shows that most transfected cells showed a shift in EC50 towards chemoresistance. According to our hypothesis, we should have expected to observe increased chemoresistance only in SW480 and SW620 transfected with miR-92a-3p-mimic, and the opposite effect in cells transfected with miR-92a-3p-inhibitor, which together would have confirmed that miR-92a-3p promotes chemoresistance.

Regardless, our results reveal a shift in all transfected cells that indicate a response to the transfection process, contrasting with previous results that reported altered cell viability because of liposome toxicity (related to Lipofectamine™ treatment) or because of transfection with microRNA mimics (related to the use of mirVana™ microRNA mimics in our study), which on the contrary has been characterized by a decrease in cell viability and proliferation[60,65]. Nevertheless, we should also keep in mind that most of the shifts in EC50 were statistically non-significant.

The multiwell MTT assay used for viability quantification of chemotherapy-exposed cells may also have limitations in determining response to 5-FU / L-OHP treatment in transfected cells. This assay determines viability by exposing the cells to an MTT solution, which is reduced to formazan by metabolically active cells. At the endpoint of this assay, the formazan crystals are solubilized, and the optical density (OD) of the solution is measured. In an ideal scenario, the OD is proportional to the percentage of viable cells in an experimental setting compared to control conditions. However, it has been reported that exposure of cells to chemo or radiotherapy caused accumulation of growth-arrested giant cells, characterized by up to 10 times higher MTT metabolization, leading to underestimation of treatment sensitivity[66,67]. This phenomenon has been attributed to a state known as senescence-associated secretory phenotype (SASP), in which cells are characterized by proliferation arrest, secretory phenotype, increased reactive oxygen species, and high metabolic activity[66]. The aberrant

changes in cell viability in transfected cells may be a result of SASP SW480 and SW620 cells interfering in the MTT assay.

One of the major challenges we faced during this research was dealing with Mycoplasma contamination in our laboratory. Indeed, several months were dedicated to treating SW480 and SW620 cell cultures with antibiotics to eliminate a resistant strain of *Mycoplasma spp*., including ciprofloxacin, tiamulin, minocycline, and gentamicin, from May to October 2021. During this period, we tested the chemosensitivity of SW480 and SW620 cells by MTT assay and found that antibiotic exposure induced chemoresistance in cell lines to 5-FU / L-OHP (results not shown), which persisted in SW480 cells even after antibiotic withdrawal. We could hypothesize that stress induced by prolonged antibiotic treatment, together with the transfection and 5-FU / L-OHP treatment-induced stress, may have caused SW480 and SW620 cells to acquire a SASP behavior.

Moreover, compared with the study by Hu *et al*. (2019) that evaluated the sensitivity of SW480 and SW620 cells to 5-FU / L-OHP treatment, we observe that our cell cultures portray some degree of chemoresistance to these drugs during antibiotic treatment[23]. In fact, chemosensitivity in our cells resembled the ones observed for SW480 and SW620 cells treated with 5-FU and L-OHP as monotherapy, indicating that any synergy from combined therapy was lost[68–71]. This phenomenon, together with the observed effect of transfection on the chemosensitivity of SW480 and SW620 cells, represents a significant limitation in our study. Single-cell observation methods like single-cell MTT or annexin-V flow cytometry are more reliable tools for determining cell viability while accounting for this event[67].

Other confounding variables that may need to be assessed include the expression of other microRNAs of the cluster miR-17~92, including miR-92a-1-5p, the 5' arm of the miR-92a precursor duplex. Unlike miR-92a-3p, the expression of miR-92a-1-5p has rarely been highlighted in the analysis of colorectal cancer and colon tissues. Increased expression of miR-92a-1-5p in normal colorectal mucosa has been associated with increased all-cause mortality in alcohol consumers, was linked to increased regorafenib toxicity in colorectal cancer patients, and was observed in an *in vitro* model of bile acid-induced gastric intestinal metaplasia in gastric cell lines[72–74].

The miR-17~92 cluster encodes six tandem microRNAs, miR-17, miR-18a, miR-19a, miR-20a, miR-19b-1, and miR-92a. The microRNAs coded in the miR-17~92 cluster are critical for embryonic and B-cell development, among other physiological functions, and therefore are expressed in practically all mouse/human tissues[75,76]. One of the main roles of the cluster is to

moderate response to TGF-β by targeting multiple proteins in the downward signaling cascade[75]. Additionally, miR-17-5p has shown to counteract some of the prooncogenic effects of miR-92a-3p, while both miR-17-5p and miR-20a-5p establish a negative feedback loop, regulating the expression of the whole cluster[75,76].

Transcription of the miR-17~92 cluster has shown to be triggered by the transcription factor c-MYC and by β-catenin/TCF transcription factors[75,77]. Although all microRNAs in the cluster are transcribed in equal amounts in the pri-miR-17~92a transcript, because of its complex tertiary structure, most of the microRNAs encoded should be suboptimal substrates for Drosha-DGCR8 processing, which is the first step in microRNA maturation[76]. Nonetheless, not only are these microRNAs correctly processed, but some of them are selectively processed over others by the intervention of trans-acting factors that are yet to be defined, and therefore the mature microRNAs in the miR-17~92 cluster are not expressed in the same ratios[76,78].

Co-expression of both 5p and 3p microRNA mature branches of miR-17, miR-18a, and 20a has been observed in colon cancer cell lines, which are also upregulated compared to their non-cancerous counterpart colon tissues. The research by Choo *et al.* (2014) suggests that there is a redundancy in the targets of 5p/3p microRNA pairs that serve as a safe-proof mechanism for the regulation of gene expression[79]. Moreover, miR-92a-3p belongs to the miR-92a/mir25 seed family together with miR-25-3p and miR-363-3p, with the seed being the first nucleotides in positions 2 to 7, counting from 5' to 3' ends in the mature microRNA sequence, which is the core determinant for target recognition of the RNA-induced silencing complex (RISC), the effector of microRNA regulation of gene expression. MiR-25-3p, miR-92a-3p, and miR-363-3p share the same seed sequence and have demonstrated to promote tumor proliferation, resistance to apoptosis, and metastasis[75,80].

In future experiments would be necessary to quantify the expression of the other members of the oncomir-1 gene and the miR-92a/mir25 seed family in response to increased or decreased miR-92-a3p levels, considering the pleiotropic and often redundant outcomes of miRNAs in gene expression. For example, lack of response to miR-92a-3p inhibitor may be hypothetically mediated by the upregulation of miR-25-3p, which has also shown to target E-cadherin expression and may affect targets in common pathways, compensating for the absence of miR-92a-3p and explaining the lack of significant differences observed in protein expression and immunofluorescence assays in our results[81].

Our research results show an inverse correlation between miR-92a-3p and the expression of *ERCC1* and *XRCC1* mRNA, both enzymes involved in DNA-repair pathways.

This last finding aligns with the research published by Zhang *et al.* (2020), where they observed low expression of *XRCC1* in ESCC tissue samples and cell lines with high expression of mesenchymal markers[54]. Recent research has revealed an intriguing link between decreased DNA repair, hypermutability, and resistance to cancer therapies (particularly targeted therapies). Common findings include decreased expression and functionality of DNA-repair complexes like mismatch repair and homologous recombination, expression of low fidelity DNA polymerases, and overall accumulation of genomic mutations that promote tumor heterogeneity over time, promoting stochastic acquisition of resistance to targeted therapies like cetuximab[82,83].

The recent discoveries by Russo *et al.* (2019) focused on the resistance to targeted therapies, and therefore they did not assess the expression or functionality of the NER and BER pathway and did not observe this same hypermutability in cell lines treated with 5-FU in their specific experimental results[82]. However, following a similar mechanism, changes in the expression of *ERCC2*, *XRCC1*, and other BER and NER enzymes may be downregulated in colorectal cancer cells after prolonged exposure to chemotherapy, as observed in mCRC patients suffering from acquired FOLFOX chemoresistance. In this phenomenon, we can hypothesize based on our results that miR-92a-3p may play as a mediator in chemoresistance development, and not a direct trigger as we previously proposed.

These results suggest that long-term upregulation of miR-92a-3p may participate in chemoresistance by downregulating the expression of *ERCC2* and *XRCC1* in colon cancer, promoting hypermutability and tumor heterogeneity. Although no direct epigenetic downregulation of these genes by miR-92a-3p has been described in microRNA databases (TargetScan 7.2™, miRDB™, TarBase 8.0™, miRPathDB 2.0™, and miRTargetLink 2.0™), regulation of other DNA repair enzymes has been documented, including ERCC3, part of the NER pathway, and XRCC5, involved in the non-homologous end-joining repair pathway for double-strand breaks.

The observed changes in the expression of *ERCC2* and *XRCC1* mRNA may implicate the regulation of transcription factors or other regulatory elements that have not been assessed in our study. For example, sirtuin 1, a class III histone deacetylase involved in chromatin organization and DNA stability, is a target of miR-92a-3p and has shown to inhibit proteasomal degradation of *XRCC1* at a protein level, leading to increased DNA damage repair and cisplatin resistance. However, these results correspond to different cellular models (human endothelial

and lung cancer cell lines) and imply an increase of *XRCC1* at a protein and not at an mRNA level, which does not coincide with our findings[84,85].

In perspective, it is clear that our experimental design holds several limitations that make it difficult to assess our hypothesis. As good as transfection of mimics and inhibitors is for delivery of microRNAs and other oligonucleotides *in vitro* and *in vivo* experiments, it has limitations in its effectivity not only for experimental assays but also for potential clinical applications of microRNA-based therapies. In the context of testing our hypothesis, a practical solution for the seemingly disruptive effect of the transfection process in cellular behavior includes using vectors for a more stable expression of microRNA or anti-microRNA oligonucleotides. This strategy would help to solve the time limit of transfection of commercial microRNA mimic and microRNA inhibitor oligonucleotides, while giving the transfected cells more time to recover their regular cell membrane structure and establish significant changes in protein expression in response to over/under-expressed microRNAs.

Current strategies of microRNA delivery for therapeutic applications are based on two main approaches: viral vectors and non-viral delivery systems. Viral vectors are useful as expression vectors for microRNAs *in vitro* and in more complex experimental strategies such as *in vivo* or organ expression of microRNAs because they allow for long-term gene expression. These include adenoviral vectors, adeno-associated viral vectors, retroviral vectors, and lentiviral vectors[86,87]. Alternatively, the construction of pCDNA3-miR and pAdTrace-miR plasmids have also been applied as a successful strategy for microRNA expression *in vitro*[88,89].

Non-viral vectors, on the other hand, are microRNA delivery systems that involve microvesicles and multiple forms of novel nanoparticles (NPs), like inorganic NPs (including gold, iron, silica, and graphene-based NPs), lipid-based nanocarriers (which include Lipofectamine™), synthetic polymeric vectors (including polyethyleneimine, polyethyleneglycol, poly(L-lysine), poly(lactide-co-glycolide) and polyurethane derived polymers), cell-derived membrane vesicles (including extracellular vesicles and apoptotic bodies) among others[65,86,87]. Nanoparticles are fine-tuned to comply with several requirements for appropriate therapeutical microRNA delivery, which include but are not limited to achieving a good microRNA load and long-term microRNA delivery, maintaining microRNA stability, good biocompatibility with the host organism/tissue/cell line, and target specificity[65,86,87].

Application of commercial expression plasmids or lentivirus-mediated expression of miR-92a-3p or anti-miR-92a-3p is a potential strategy for testing our hypothesis, although it implies the challenge of designing an optimal pre-microRNA sequence and controlling the

effects of lentiviral infection in cell viability and proliferation. Also, we would need to control for the expression of non-desired miR-92a-1-5p, and the correct loading of mir-92a-3p in the RISC complex.

Nanoparticle carriers can be developed for controlled delivery of miR-92a-3p delivery and could even be designed to be compatible with plasmid vectors or commercially pre-designed microRNA mimic and inhibitor oligonucleotides such as the ones used in this study, which have already solved the problems of undesired miR-92a-1-5p expression and correct miR-92a-3p-RISC loading, but still have the limitations previously discussed for mimic oligonucleotides[90]. Ultimately, we would need to verify that these nanoparticles do not cause membrane integrity disturbances like the ones observed with Lipofectamine™.

An alternative strategy to assess the role of miR-92a-3p in chemoresistance development would be to induce resistance to 5-FU / L-OHP in SW480 and SW620 cells by exposure to increasing concentrations of these drugs, and compare the expression of miR-92a-3p and our genes of interest in these resistant cell lines compared to non-resistant cells, as proposed by Virag *et al*. (2013)[91]. This strategy would have potentially unveiled an overexpression of miR-92a-3p in resistant SW480 and SW620 cells, phenotypical changes in cancer cells potentially related to EMT, and the response of these resistant cells to miR-92a-3p inhibition. This strategy has its own limitations, as it is more difficult to establish a direct causality of miR-92a-3p in chemoresistance through this proposed experimental design.

In summary, our experiments revealed that decreasing levels of miR-92a-3p led to upregulation of mRNA levels of E-cadherin, *ZEB1*, and *ERCC2* while increasing levels of miR-92a-3p downregulated β-catenin and *XRCC1* mRNA in transfected SW480 and SW620 cell lines. These changes in mRNA expression, unfortunately, did not reflect in the protein levels of these genes. We failed to observe changes in morphology, β-catenin distribution, or other evidence of EMT that could be linked with changes in levels of miR-92a-3p in SW480 and SW620 cell lines. Therefore, based on our results, we cannot confirm that an increase in miR-92a-3p levels is enough to trigger EMT or modify the expression of *DPYD*, *TYMS*, *MTHFR*, *ERCC1*, *ERCC2*, and *XRCC1* proteins.

Our results also suggest that miR-92a-3p may reduce the sensitivity of SW480 cells to 5-FU / L-OHP. However, because of similar effects observed in cells treated with negative control, and the poor goodness of fit in our dose-response curves (expressed by the low R^2 values in Table 1) we cannot confirm our hypothesis based on our results. Limitations of our experimental model need to be overrun before discarding a potential association.

The purpose of this research was to assess the role of mir-92a-3p in the activation of β-catenin and the EMT program in tumor cells and describe a mechanism of chemoresistance of tumor cells that involves the expression of genes that predict 5-FU-based chemotherapy response in the clinical practice. We expected to find a novel mechanism of tumor resistance that implied the connection between two phenomena that, to date, have been mostly studied as part of independent areas of scientific research, which are the expression of pharmacogenetic biomarkers and EMT.

Previous research showed substantial interest in assessing the role of mir-92a-3p on tumoral cells and stroma in CRC progression[23,24,94,25–28,61,62,92,93]. Significant efforts are being made to establish potential biomarker microRNAs for cancer diagnosis and disease progression, which goes hand-to-hand with the rapid development of new microRNA quantification tools that may allow less invasive screening during disease evolution and promising therapeutic targets in the fight against cancer[65,87,95,96].

Although our results suggest that miR-92a-3p has no impact on chemoresistance by modifying the expression of pharmacogenomic biomarkers of FOLFOX response in CRC cell lines, the potential role of other microRNAs deserves to be explored. This includes microRNAs such as miR-21, miR-23b, miR-125b-5p, and miR-210, which have demonstrated to induce EMT in CRC cell lines[12]. In the future, circulating microRNAs may be established as novel pharmacogenetic tools to assess 5-FU-based chemotherapy sensitivity.

CONCLUSIONS

- Based on our experimental results, we can establish that transient increase of miR-92a-3p does not lead to the activation of β-catenin in SW480 and SW620 cell lines but modifies the expression of E-cadherin, β-catenin, and *ZEB1* mRNA, suggesting an early step in EMT activation.
- Increased levels of miR-92a-3p downregulate the expression of *ERCC2* mRNA and decreased levels of miR-92a-3p upregulate the expression of *XRCC1* mRNA in SW620 cells *in vitro*, suggesting that miR-92a-3p may regulate of expression of these DNA repair-complex subunits.
- Changes in miR-92a-3p did not exert significant effects on mRNA expression of *SNAIL*, *SLUG*, vimentin, *DPYD*, *TYMS*, *MTHFR*, or *ERCC1* in SW480 and SW620 cell lines.
- We cannot establish if miR-92a-3p has an effect on the chemosensitivity of SW480 and SW620 cells to 5-FU and L-OHP treatment *in vitro*.

ARTICLES PUBLISHED IN PEER-REVIEWED JOURNALS DURING THE DEVELOPMENT OF THE THESIS PROJECT:

- Escalante PI, Quiñones LA, Contreras HR. Epithelial-Mesenchymal Transition and MicroRNAs in Colorectal Cancer Chemoresistance to FOLFOX. *Pharmaceutics.* 2021; 13(1):75. https://doi.org/10.3390/pharmaceutics13010075. IF 2020: 6.321

REFERENCE LIST

1. Siegel RL, Miller KD, Fuchs HE, Jemal A. Cancer statistics, 2022. *CA Cancer J Clin*. 2022;72(1):7-33. doi:10.3322/CAAC.21708
2. Siegel RL, Miller KD, Goding Sauer A, et al. Colorectal cancer statistics, 2020. *CA Cancer J Clin*. Published online March 5, 2020:caac.21601. doi:10.3322/caac.21601
3. American Cancer Society. Colorectal Cancer Facts & Figures 2020-2022.
4. Holmes D. A disease of growth. *Nature*. 2015;521(7551):S2-S3. doi:10.1038/521S2a
5. Ministerio de Salud C. *Guía Clínica AUGE Cáncer Colorrectal*.; 2013. Accessed April 20, 2020. https://www.minsal.cl/portal/url/item/db8329dc44e6371de0400101640126b5.pdf
6. Ministerio de Salud C. *Estrategia Nacional de Cáncer*.; 2016. Accessed April 20, 2020. https://www.minsal.cl/wp-content/uploads/2016/10/Estrategia-Nacional-de-Cancer-version-consulta-publica.pdf
7. Weisenberg E. Pathology Outlines - TNM staging of colorectal carcinoma (AJCC 8th edition). Accessed April 20, 2020. http://www.pathologyoutlines.com/topic/colontumorstaging8ed.html
8. Ismaili N. Treatment of colorectal liver metastases. *World J Surg Oncol*. 2011;9(1):154. doi:10.1186/1477-7819-9-154
9. Van Cutsem E, Cervantes A, Adam R, et al. ESMO consensus guidelines for the management of patients with metastatic colorectal cancer. *Ann Oncol*. 2016;27(8):1386-1422. doi:10.1093/annonc/mdw235
10. Edwards MS, Chadda SD, Zhao Z, Barber BL, Sykes DP. A systematic review of treatment guidelines for metastatic colorectal cancer. *Color Dis*. 2012;14(2):e31-e47. doi:10.1111/j.1463-1318.2011.02765.x
11. Hammond WA, Swaika A, Mody K. Pharmacologic resistance in colorectal cancer: A review. *Ther Adv Med Oncol*. 2016;8(1):57-84. doi:10.1177/1758834015614530

12. Escalante PI, Quiñones LA, Contreras HR. Epithelial-Mesenchymal Transition and MicroRNAs in Colorectal Cancer Chemoresistance to FOLFOX. *Pharm 2021, Vol 13, Page 75*. 2021;13(1):75. doi:10.3390/pharmaceutics
13. Vessoni AT, Filippi-Chiela EC, Lenz G, Batista LFZ. Tumor propagating cells: drivers of tumor plasticity, heterogeneity, and recurrence. *Oncogene*. 2020;39(10):2055-2068. doi:10.1038/s41388-019-1128-4
14. Le Magnen C, Shen MM, Abate-Shen C. Lineage Plasticity in Cancer Progression and Treatment. *Annu Rev Cancer Biol*. 2018;2:271-289. doi:10.1146/annurev-cancerbio-030617-050224
15. Lu W, Kang Y. Epithelial-Mesenchymal Plasticity in Cancer Progression and Metastasis. *Dev Cell*. 2019;49(3):361-374. doi:10.1016/j.devcel.2019.04.010
16. Hanahan D. Hallmarks of Cancer: New Dimensions. *Cancer Discov*. 2022;12(1):31-46. doi:10.1158/2159-8290.CD-21-1059
17. Celià-Terrassa T, Jolly MK. Cancer Stem Cells and Epithelial-to-Mesenchymal Transition in Cancer Metastasis. *Cold Spring Harb Perspect Med*. Published online September 30, 2019:a036905. doi:10.1101/cshperspect.a036905
18. Brembeck FH, Rosário M, Birchmeier W. Balancing cell adhesion and Wnt signaling, the key role of β-catenin. *Curr Opin Genet Dev*. 2006;16(1):51-59. doi:10.1016/j.gde.2005.12.007
19. Valenta T, Hausmann G, Basler K. The many faces and functions of Î 2-catenin. *EMBO J*. 2012;31(12):2714-2736. doi:10.1038/emboj.2012.150
20. Gonzalez DM, Medici D. Signaling mechanisms of the epithelial-mesenchymal transition. *Sci Signal*. 2014;7(344):re8. doi:10.1126/scisignal.2005189
21. Quail DF, Joyce JA. Microenvironmental regulation of tumor progression and metastasis. *Nat Med*. 2013;19(11):1423-1437. doi:10.1038/nm.3394
22. Klemm F, Joyce JA. Microenvironmental regulation of therapeutic response in cancer. *Trends Cell Biol*. 2015;25(4):198-213. doi:10.1016/j.tcb.2014.11.006
23. Hu JL, Wang W, Lan XL, et al. CAFs secreted exosomes promote metastasis and chemotherapy resistance by enhancing cell stemness and epithelial-mesenchymal transition in colorectal cancer. *Mol Cancer*. 2019;18(1). doi:10.1186/s12943-019-1019-x
24. Li X, Guo S, Min L, Guo Q, Zhang S. MiR-92a-3p promotes the proliferation, migration and invasion of esophageal squamous cell cancer by regulating PTEN. *Int J Mol Med*. 2019;44(3):973-981. doi:10.3892/ijmm.2019.4258

25. Song H, Zhang Y, Liu N, Zhao S, Kong Y, Yuan L. MiR-92a-3p exerts various effects in glioma and glioma stem-like cells specifically targeting CDH1/β-catenin and notch-1/Akt signaling pathways. *Int J Mol Sci*. 2016;17(11). doi:10.3390/ijms17111799
26. Chen ZL, Zhao XH, Wang JW, et al. microRNA-92a promotes lymph node metastasis of human esophageal squamous cell carcinoma via E-cadherin. *J Biol Chem*. 2011;286(12):10725-10734. doi:10.1074/JBC.M110.165654
27. Zhang G, Zhou H, Xiao H, Liu Z, Tian H, Zhou T. MicroRNA-92a functions as an oncogene in colorectal cancer by targeting PTEN. *Dig Dis Sci*. 2014;59(1):98-107. doi:10.1007/S10620-013-2858-8
28. Ke TW, Wei PL, Yeh KT, Chen WTL, Cheng YW. MiR-92a Promotes Cell Metastasis of Colorectal Cancer Through PTEN-Mediated PI3K/AKT Pathway. *Ann Surg Oncol*. 2015;22(8):2649-2655. doi:10.1245/s10434-014-4305-2
29. Persad A, Venkateswaran G, Hao L, et al. Active β-catenin is regulated by the PTEN/PI3 kinase pathway: A role for protein phosphatase PP2A. *Genes and Cancer*. 2016;7(11-12):368-382. doi:10.18632/genesandcancer.128
30. Jiang J xin, Sun C yi, Tian S, Yu C, Chen M yuan, Zhang H. Tumor suppressor Fbxw7 antagonizes WNT signaling by targeting β-catenin for degradation in pancreatic cancer. *Tumor Biol*. 2016;37(10):13893-13902. doi:10.1007/s13277-016-5217-5
31. López-Cortés A, Paz-y-Miño C, Guerrero S, et al. Pharmacogenomics, biomarker network, and allele frequencies in colorectal cancer. *Pharmacogenomics J*. 2020;20(1):136-158. doi:10.1038/s41397-019-0102-4
32. Quiñones L, Roco Á, Cayún JP, et al. Clinical applications of pharmacogenomics. *Rev Med Chil*. 2017;145(4). doi:10.4067/S0034-98872017000400009
33. Weinshilboum RM, Wang L. Pharmacogenomics: Precision Medicine and Drug Response. *Mayo Clin Proc*. 2017;92(11):1711-1722. doi:10.1016/j.mayocp.2017.09.001
34. Guy JW, Patel I, Oestreich JH. Clinical Application and Educational Training for Pharmacogenomics. *Pharmacy*. 2020;8(3):163. doi:10.3390/pharmacy8030163
35. Jakobsen A, Nielsen JN, Gyldenkerne N, Lindeberg J. Thymidylate synthase and methylenetetrahydrofolate reductase gene polymorphism in normal tissue as predictors of fluorouracil sensitivity. *J Clin Oncol*. 2005;23(7):1365-1369. doi:10.1200/JCO.2005.06.219
36. Longley DB, Harkin DP, Johnston PG. 5-Fluorouracil: Mechanisms of action and clinical strategies. *Nat Rev Cancer*. 2003;3(5):330-338. doi:10.1038/nrc1074

37. Quiñones L, Roco Á, Cayún JP, et al. Farmacogenómica como herramienta fundamental para la medicina personalizada: Aplicaciones en la práctica clínica. *Rev Med Chil*. 2017;145(4):483-500. doi:10.4067/S0034-98872017000400009
38. Di Francia R, De Lucia L, Di Paolo M, et al. Rational selection of predictive pharmacogenomics test for the Fluoropyrimidine/Oxaliplatin based therapy. *Eur Rev Med Pharmacol Sci*. 2015;19(22):4443-4454. Accessed April 22, 2020. https://pubmed.ncbi.nlm.nih.gov/26636535/
39. Gnoni A, Russo A, Silvestris N, et al. Pharmacokinetic and Metabolism Determinants of Fluoropyrimidines and Oxaliplatin Activity in Treatment of Colorectal Patients. *Curr Drug Metab*. 2011;12(10):918-931. doi:10.2174/138920011798062300
40. Marsh S, McLeod H, Dolan E, et al. Platinum pathway. *Pharmacogenet Genomics*. 2009;19(7):563-564. doi:10.1097/FPC.0b013e32832e0ed7
41. Alcindor T, Beauger N. Oxaliplatin: a review in the era of molecularly targeted therapy. *Curr Oncol*. 2011;18(1):18. doi:10.3747/CO.V18I1.708
42. Aiello M, Vella N, Cannavò C, et al. Role of genetic polymorphisms and mutations in colorectal cancer therapy (Review). *Mol Med Rep*. 2011;4(2):203-208. doi:10.3892/mmr.2010.408
43. Slyskova J, Sabatella M, Ribeiro-Silva C, et al. Base and nucleotide excision repair facilitate resolution of platinum drugs-induced transcription blockage. *Nucleic Acids Res*. 2018;46(18):9537. doi:10.1093/NAR/GKY764
44. Paré L, Marcuello E, Altés A, et al. Pharmacogenetic prediction of clinical outcome in advanced colorectal cancer patients receiving oxaliplatin/5-fluorouracil as first-line chemotherapy. *Br J Cancer*. 2008;99(7):1050-1055. doi:10.1038/sj.bjc.6604671
45. Du B, Shim JS. Targeting Epithelial–Mesenchymal Transition (EMT) to Overcome Drug Resistance in Cancer. *Molecules*. 2016;21(7). doi:10.3390/MOLECULES21070965
46. Zhu W-P, Liu Z-Y, Zhao Y-M, et al. Dihydropyrimidine dehydrogenase predicts survival and response to interferon-α in hepatocellular carcinoma. *Cell Death Dis*. 2018;9(2):69. doi:10.1038/s41419-017-0098-0
47. Shaul YD, Freinkman E, Comb WC, et al. Dihydropyrimidine accumulation is required for the epithelial-mesenchymal transition. *Cell*. 2014;158(5):1094-1109. doi:10.1016/j.cell.2014.07.032
48. Siddiqui A, Vazakidou ME, Schwab A, et al. Thymidylate synthase is functionally associated with ZEB1 and contributes to the epithelial-to-mesenchymal transition of cancer cells. *J Pathol*. 2017;242(2):221-233. doi:10.1002/path.4897

49. Ahn J-Y, Lee J-S, Min H-Y, Lee H-Y. Acquired resistance to 5-fluorouracil via HSP90/Src-mediated increase in thymidylate synthase expression in colon cancer. *Oncotarget*. 2015;6(32):32622-32633. doi:10.18632/oncotarget.5327
50. Sakowicz-Burkiewicz M, Przybyla T, Wesserling M, Bielarczyk H, Maciejewska I, Pawelczyk T. Suppression of TWIST1 enhances the sensitivity of colon cancer cells to 5-fluorouracil. *Int J Biochem Cell Biol*. 2016;78:268-278. doi:10.1016/j.biocel.2016.07.024
51. Wei W, Ma X-D, Jiang G-M, et al. The AKT/GSK3β mediated Slug expression contributes to oxaliplatin resistance in 4 colorectal cancer via up-regulation of ERCC1. *Oncol Res Featur Preclin Clin Cancer Ther*. 2020;28(4). doi:10.3727/096504020x15877284857868
52. Wu Y, Jin D, Wang X, et al. UBE2C Induces Cisplatin Resistance via ZEB1/2-Dependent Upregulation of ABCG2 and ERCC1 in NSCLC Cells. *J Oncol*. 2019;2019. doi:10.1155/2019/8607859
53. Hsu DSS, Lan HY, Huang CH, et al. Regulation of excision repair cross-complementation group 1 by snail contributes to cisplatin resistance in head and neck cancer. *Clin Cancer Res*. 2010;16(18):4561-4571. doi:10.1158/1078-0432.CCR-10-0593
54. Zhang Z, Li X, Xiong F, Ren Z, Han Y. Hsa_circ_0012563 promotes migration and invasion of esophageal squamous cell carcinoma by regulating XRCC1/EMT pathway. *J Clin Lab Anal*. 2020;34(8). doi:10.1002/jcla.23308
55. Li Q, Zhou X, Fang Z, Pan Z. Effect of STC2 gene silencing on colorectal cancer cells. *Mol Med Rep*. 2019;20(2):977-984. doi:10.3892/MMR.2019.10332/HTML
56. Coghlan MP, Culbert AA, Cross DAE, et al. Selective small molecule inhibitors of glycogen synthase kinase-3 modulate glycogen metabolism and gene transcription. *Chem Biol*. 2000;7(10):793-803. doi:10.1016/S1074-5521(00)00025-9
57. Lee SC, Kim OH, Lee SK, Kim SJ. IWR-1 inhibits epithelial-mesenchymal transition of colorectal cancer cells through suppressing Wnt/β-catenin signaling as well as survivin expression. *Oncotarget*. 2015;6(29):27146. doi:10.18632/ONCOTARGET.4354
58. Tran FH, Zheng JJ. Modulating the wnt signaling pathway with small molecules. *Protein Sci*. 2017;26(4):650. doi:10.1002/PRO.3122
59. Nachar N. The Mann-Whitney U: A Test for Assessing Whether Two Independent Samples Come from the Same Distribution. *Tutor Quant Methods Psychol*. 2008;4(1):13-20. doi:10.20982/TQMP.04.1.P013

60. Jin HY, Gonzalez-Martin A, Miletic A V., et al. Transfection of microRNA mimics should be used with caution. *Front Genet*. 2015;6(DEC):340. doi:10.3389/FGENE.2015.00340/BIBTEX
61. Zhu S, Zhang L, Zhao Z, et al. MicroRNA-92a-3p inhibits the cell proliferation, migration and invasion of Wilms tumor by targeting NOTCH1. *Oncol Rep*. 2018;40(2):571-578. doi:10.3892/or.2018.6458
62. Liao G, Xiong H, Tang J, Li Y, Liu Y. MicroRNA-92a Inhibits the Cell Viability and Metastasis of Prostate Cancer by Targeting SOX4: *https://doi.org/101177/1533033820959354*. 2020;19. doi:10.1177/1533033820959354
63. Reliable stable expression Lipofectamine ™ 2000 Reagent. Accessed May 31, 2022. www.invitrogen.com
64. Fuge G, Zeng AP, Jandt U. Weak cell cycle dependency but strong distortive effects of transfection with Lipofectamine 2000 in near-physiologically synchronized cell culture. *Eng Life Sci*. 2017;17(4):348. doi:10.1002/ELSC.201600113
65. Lee SWL, Paoletti C, Campisi M, et al. MicroRNA delivery through nanoparticles. *J Control Release*. 2019;313:80-95. doi:10.1016/j.jconrel.2019.10.007
66. Ghasemi M, Turnbull T, Sebastian S, Kempson I. The mtt assay: Utility, limitations, pitfalls, and interpretation in bulk and single-cell analysis. *Int J Mol Sci*. 2021;22(23). doi:10.3390/IJMS222312827/S1
67. Mirzayans R, Andrais B, Murray D. Molecular Sciences Do Multiwell Plate High Throughput Assays Measure Loss of Cell Viability Following Exposure to Genotoxic Agents? Published online 2017. doi:10.3390/ijms18081679
68. Wu H, Liang Y, Shen L, Shen L. MicroRNA-204 modulates colorectal cancer cell sensitivity in response to 5-fluorouracil-based treatment by targeting high mobility group protein A2. *Biol Open*. 2016;5(5):563-570. doi:10.1242/bio.015008
69. Hua Y, Zhu Y, Zhang J, et al. miR-122 Targets X-Linked Inhibitor of Apoptosis Protein to Sensitize Oxaliplatin-Resistant Colorectal Cancer Cells to Oxaliplatin-Mediated Cytotoxicity. *Cell Physiol Biochem*. 2018;51(5):2148-2159. doi:10.1159/000495832
70. Chai J, Dong W, Xie C, et al. MicroRNA-494 sensitizes colon cancer cells to fluorouracil through regulation of DPYD. *IUBMB Life*. 2015;67(3):191-201. doi:10.1002/iub.1361
71. Chai H, Liu M, Tian R, Li X, Tang H. miR-20a targets BNIP2 and contributes chemotherapeutic resistance in colorectal adenocarcinoma SW480 and SW620 cell lines. *Acta Biochim Biophys Sin (Shanghai)*. 2011;43(3):217-225.

doi:10.1093/abbs/gmq125

72. Mullany LE, Herrick JS, Wolff RK, Stevens JR, Slattery ML. Alterations in microRNA expression associated with alcohol consumption in rectal cancer subjects. 2017;28:545-555. doi:10.1007/s10552-017-0882-2
73. Conde E, Earl J, Crespo-Toro L, et al. Biomarkers Associated with Regorafenib First-Line Treatment Benefits in Metastatic Colorectal Cancer Patients: REFRAME Molecular Study. *Cancers (Basel)*. 2021;13(7). doi:10.3390/CANCERS13071710
74. li ting, guo H, li H, et al. MicroRNA-92a-1-5p increases CDX2 by targeting FOXD1 in bile acids-induced gastric intestinal metaplasia. *Gut*. 2019;68:1751-1763. doi:10.1136/gutjnl-2017-315318
75. Concepcion CP, Bonetti C, Ventura A. The microRNA-17-92 family of microRNA clusters in development and disease. *Cancer J*. 2012;18(3):262-267. doi:10.1097/PPO.0B013E318258B60A
76. Chakraborty S, Krishnan Y. A structural map of oncomiR-1 at single-nucleotide resolution. *Nucleic Acids Res*. 2017;45(16):9694–9705. doi:10.1093/nar/gkx613
77. Li Y, Lauriola M, Kim D, et al. Adenomatous polyposis coli (APC) regulates miR17-92 cluster through β-catenin pathway in colorectal cancer. *Oncogene*. 2016;35(35):4558-4568. doi:10.1038/ONC.2015.522
78. Chaulk SG, Thede GL, Kent OA, et al. Role of pri-miRNA tertiary structure in miR-17∼92 miRNA biogenesis. *RNA Biol*. 2011;8(6). doi:10.4161/rna.8.6.17410
79. Choo KB, Soon YL, Nguyen PNN, Hiew MSY, Huang CJ. MicroRNA-5p and -3p co-expression and cross-targeting in colon cancer cells. *J Biomed Sci*. 2014;21(1). doi:10.1186/S12929-014-0095-X
80. Li M, Guan X, Sun Y, et al. miR-92a family and their target genes in tumorigenesis and metastasis. *Exp Cell Res*. 2014;323(1):1-6. doi:10.1016/J.YEXCR.2013.12.025
81. Xu X, Chen Z, Zhao X, et al. MicroRNA-25 promotes cell migration and invasion in esophageal squamous cell carcinoma. *Biochem Biophys Res Commun*. 2012;421(4):640-645. doi:10.1016/J.BBRC.2012.03.048
82. Russo M, Crisafulli G, Sogari A, et al. Adaptive mutability of colorectal cancers in response to targeted therapies. *Science (80-)*. 2019;366(6472):1473-1480. doi:10.1126/science.aav4474
83. Gay CM, Parseghian CM, Byers LA. This Is Our Cells Under Pressure: Decreased DNA Damage Repair in Response to Targeted Therapies Facilitates the Emergence of Drug-Resistant Clones. *Cancer Cell*. 2020;37(1):5-7.

doi:10.1016/J.CCELL.2019.12.005

84. Chen Z, Wen L, Martin M, et al. Oxidative stress activates endothelial innate immunity via sterol regulatory element binding protein 2 (SREBP2) transactivation of microRNA-92a. *Circulation*. 2015;131(9):805-814. doi:10.1161/CIRCULATIONAHA.114.013675
85. Yousafzai NA, Zhou Q, Xu W, et al. SIRT1 deacetylated and stabilized XRCC1 to promote chemoresistance in lung cancer. *Cell Death Dis*. 2019;10(5). doi:10.1038/S41419-019-1592-3
86. Fu Y, Chen J, Huang Z. Recent progress in microRNA-based delivery systems for the treatment of human disease. *ExRNA 2019 11*. 2019;1(1):1-14. doi:10.1186/S41544-019-0024-Y
87. Ganju A, Khan S, Hafeez BB, et al. miRNA nanotherapeutics for cancer. doi:10.1016/j.drudis.2016.10.014
88. Fan J, Feng Y, Zhang R, et al. A simplified system for the effective expression and delivery of functional mature microRNAs in mammalian cells. *Cancer Gene Ther 2019 276*. 2019;27(6):424-437. doi:10.1038/s41417-019-0113-y
89. Morales-Pison S, Carrasco V, Gutiérrez-Vera C, et al. Genetic Variation in MicroRNA-423 Promotes Proliferation, Migration, Invasion, and Chemoresistance in Breast Cancer Cells. *Int J Mol Sci*. 2021;23(1). doi:10.3390/IJMS23010380
90. Thomson DW, Bracken CP, Szubert JM, Goodall GJ. On Measuring miRNAs after Transient Transfection of Mimics or Antisense Inhibitors. *PLoS One*. 2013;8(1):e55214. doi:10.1371/JOURNAL.PONE.0055214
91. Virag P, Fischer-Fodor E, Perde-Schrepler M, et al. Oxaliplatin induces different cellular and molecular chemoresistance patterns in colorectal cancer cell lines of identical origins. *BMC Genomics*. 2013;14(1):1. doi:10.1186/1471-2164-14-480
92. Tsuchida A, Ohno S, Wu W, et al. miR-92 is a key oncogenic component of the miR-17-92 cluster in colon cancer. *Cancer Sci*. 2011;102(12):2264-2271. doi:10.1111/j.1349-7006.2011.02081.x
93. Fu F, Jiang W, Zhou L, Chen Z. Circulating Exosomal miR-17-5p and miR-92a-3p Predict Pathologic Stage and Grade of Colorectal Cancer. *Transl Oncol*. 2018;11(2):221-232. doi:10.1016/j.tranon.2017.12.012
94. Wei Q-D, Zheng W-B, Sun K, Xue Q, Yang C-Z, Li G-X. MiR-92a promotes the invasion and migration of colorectal cancer by targeting RECK. *Int J Clin Exp Pathol*. 2019;12(5):1565-1577. Accessed July 15, 2020. http://www.ncbi.nlm.nih.gov/pubmed/31933974

95. Bakhsh T, Alhazmi S, Alburae NA, et al. Exosomal miRNAs as a Promising Source of Biomarkers in Colorectal Cancer Progression. *Int J Mol Sci*. 2022;23(9). doi:10.3390/IJMS23094855
96. Masuda T, Hayashi N, Kuroda Y, Ito S, Eguchi H, Mimori K. MicroRNAs as biomarkers in colorectal cancer. *Cancers (Basel)*. 2017;9(9). doi:10.3390/cancers9090124

APPENDICES

Appendix 1

Table 3: Primer sequences used for RT-qPCR analysis.

Gene	Forward primer (5'-3')	Reverse primer (5'-3')
SNAIL	GAG CTG CAG GAC TCT AAT CCA GAG	AGC CTG GAG ATC CTT GGC CTC AG
SLUG	CAA GGA ATA TGT GAG CCT GGG CG	TCA GTG TGC TAC ACA GCA GCC A
TWIST1	GGA GTC CGC AGT CTT ACG AG	TCT GGA GGA CCT GGT AGA GG
ZEB1	GAT GAT GAA TGC GAG TCA GAT GC	ACA GCA GTG TCT TGT TGT TGT
E-cadherin	TCC CAA CTC CTC TCC TGG CCT	GAG GCT CTG TCA CCT TCA GCC A
β-catenin	CGA GCT GCT ATG TTC CCT GA	TCA GCC AAA CGC TGG ACA TT
Vimentin	TGG ACC AGC TAA CCA ACG AC	GCC AGA GAC GCA TTG TCA AC
N-cadherin	GGA CAG TTC CTG AGG GAT CA	GGA TTG CCT TCC ATG TCT GT
DPYD	CCG AGA AGC AAT GAG ATG CCT	ACA CAA AGA TCA GAG GTT GGA CA
TYMS	TGG GGC AGA TCC AAC ACA TC	TTT GTG GAT CCC TTG ATA AAC CAC
MTHFR	GGC CAT CTG CAC AAA GCT AAG	AAC TCA CTT CGG ATG TGC TTC AC
ERCC1	TTG GCG ACG TAA TTC CCG ACT AT	TTC ACA TCC ACC TGG ACA AGC AG
ERCC2	CTT GCT CGA TAC TCA ATC CTG C	ATG GAG TCG ATG CAG ACG TT
XRCC1	GGC AGA CAC TTA CCG AAA ATG G	GGA CAT GAA AGA TGA GGT GAC CA
Pumilio	CGG TCG TCC TGA GGA TAA AA	CGT ACG TGA GGC GTG AGT AA

Appendix 2

Table 4: Antibodies used for western blot analysis.

Antibody	Brand	Catalogue	Dilution
PRIMARY ANTIBODIES			
E-cadherin	BD Transduction Laboratories	610181	1:1000
β-catenin	BD Transduction Laboratories	610154	1:1000
Active β-catenin	Millipore	05-665	1:1000
ERCC2	Cell Signalling	11963S	1:2000
XRCC1	Cell Signalling	2735S	1:500
SECONDARY ANTIBODIES			
Goat anti-Mouse IgG HRP	Jackson Immunoresearch	115-0335-003	1:10.000
Goat anti-Rabbit IgG HRP	Jackson Immunoresearch	111-035-003	1:10.000

Appendix 3

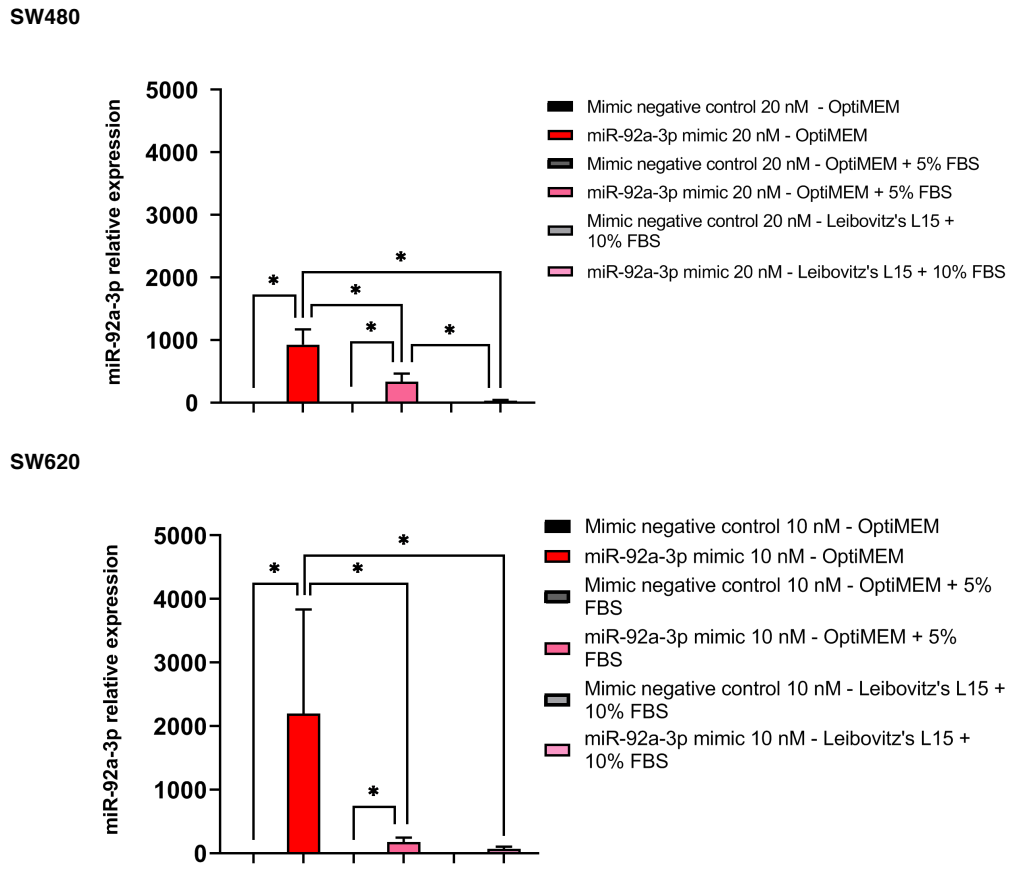

Appendix 3. Transfection efficiency curve in SW480 and SW620 cell lines transfected with miR-92a-3p mimic in supplemented culture medium: RT-qPCR analysis showing the relative expression of miR-92a-3p in SW480 and SW620 cells transfected with mimic miR-92a-3p or negative control under three different conditions: transfection with unsupplemented Opti-MEM™; transfection with Opti-MEM™ supplemented with 5% FBS 5 hours after transfection; or transfection with miR-92a-3p-mimic using Opti-MEM™ followed by change of culture medium to Leibovitz's L-15 supplemented with 10% FBS 5 hours after. Statistical differences in miR levels were determined using the Mann-Whitney U test (*p=0.05). Data represent the means ± SEM from three independent experiments.

Appendix 4

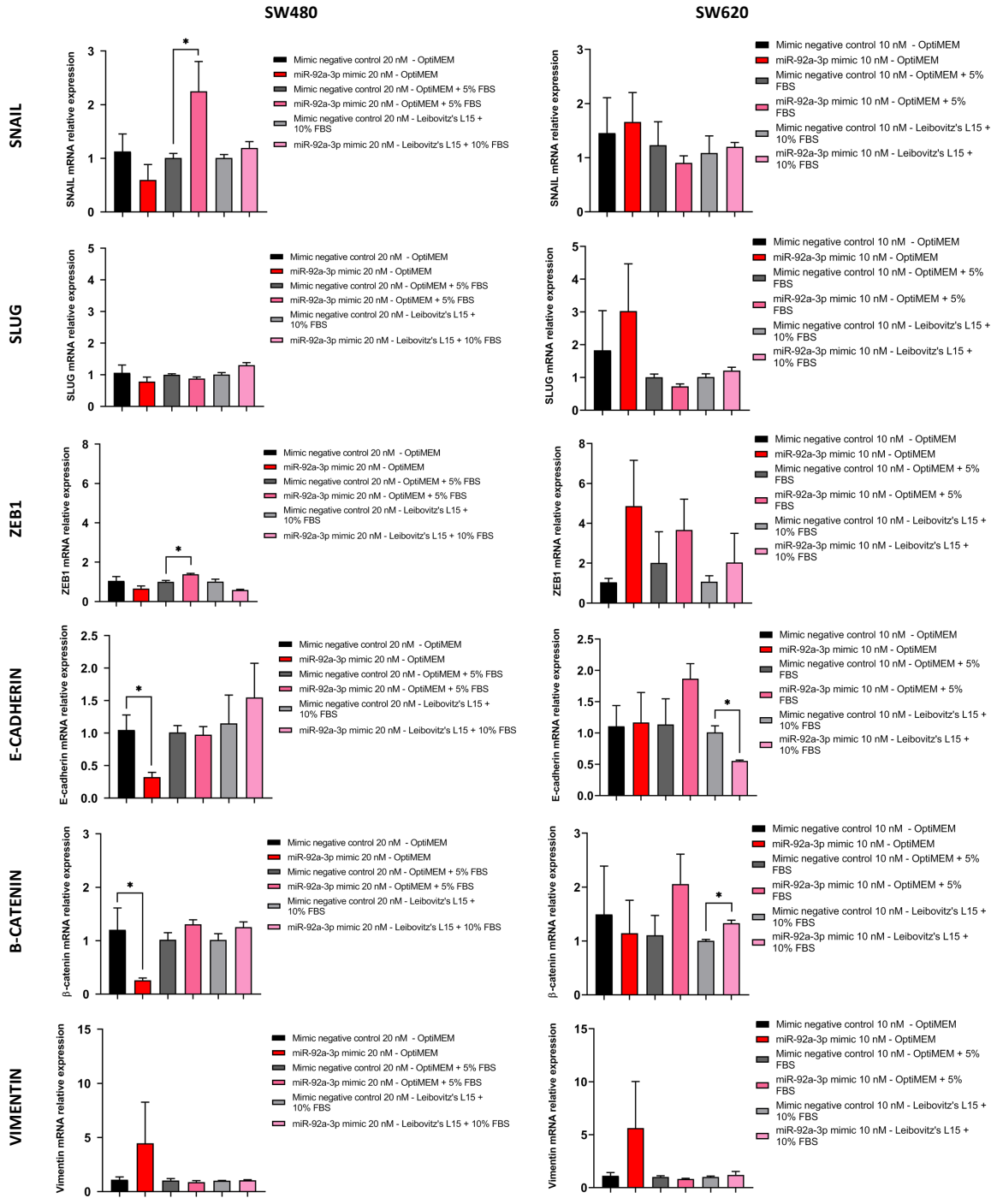

Appendix 4. Expression of EMT-Transcription factors and EMT markers in SW480 and SW620 cell lines transfected with miR-92a-3p-mimics in supplemented culture medium: RT-qPCR analysis showing the relative expression of *SNAIL*, *SLUG*, *ZEB1*, E-cadherin, β-catenin, and Vimentin mRNA upon miR-92a-3p mimic transfection in SW480 and SW620 cells under three different conditions: transfection with unsupplemented Opti-MEM™; transfection with Opti-MEM™ supplemented with 5% FBS 5 hours after transfection; or transfection with miR-92a-3p-mimic using Opti-MEM™ followed by change of culture medium to Leibovitz's L-15 supplemented with 10% FBS

5 hours after. Statistical differences in mRNA levels were determined using the Mann-Whitney U test. Data represent the means ± SEM from three independent experiments ($p>0.05$ for all experiments).

Appendix 5

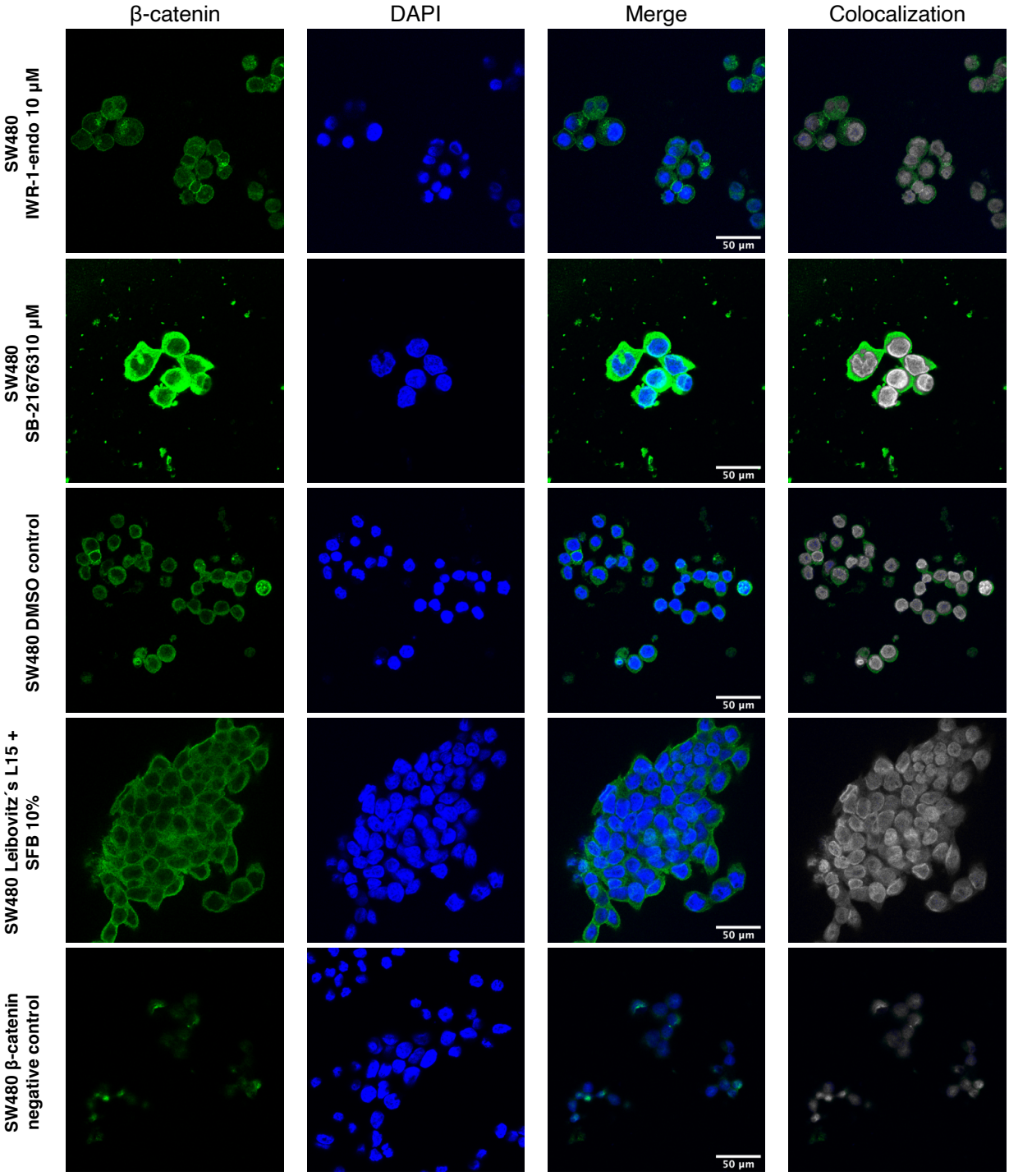

Appendix 5: Expression and β-catenin subcellular localization in response to miR-92a-3p in SW480 cells: 20.000 SW480 cells per well were seeded and after treated with IWR-1-endo 10 µM, SB-216763 10 µM, or maintained in Leibovitz´s L15 + SFB 10 for 24 hours as control, then fixed and examined by immunofluorescence for β-catenin (green), and DAPI (blue) for the nuclei as reference. Antibody negative control was performed with SW480 cells untreated in Opti-MEM™ culture medium for 24 h. Colocalization images were constructed using the Colocalization Threshold tool, indicating areas of green and blue fluorescence signal overlapping (grey).

Appendix 6

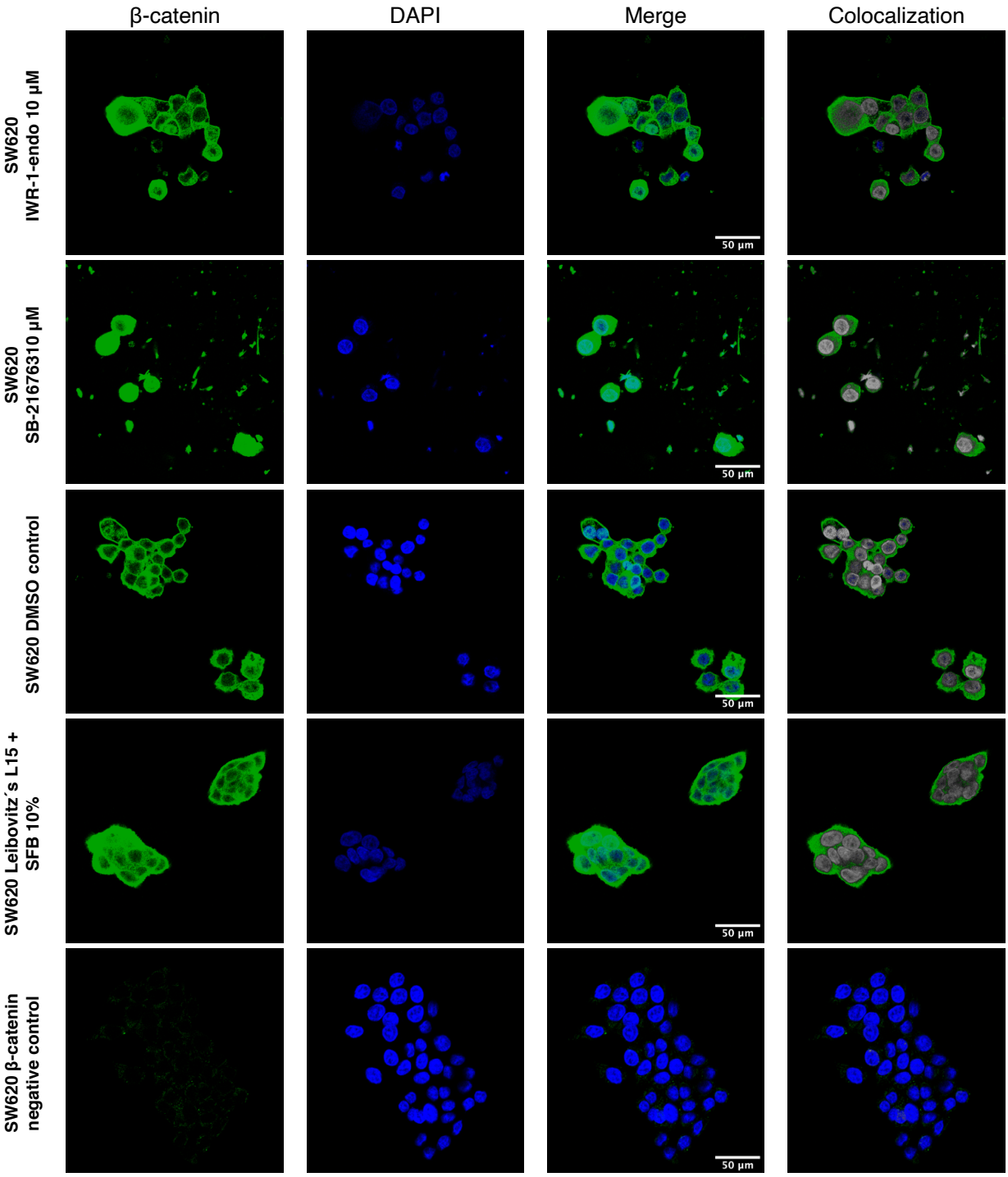

Appendix 6: Expression and β-catenin subcellular localization in response to miR-92a-3p in SW620 cells: 20.000 SW620 cells per well were seeded and after treated with IWR-1-endo 10 µM, SB-216763 10 µM, DMSO 0.81 µL/mL, or maintained in Leibovitz´s L15 + SFB 10 for 24 hours as control, then fixed and examined by immunofluorescence for β-catenin (green), and DAPI (blue) for the nuclei as reference. Antibody negative control was performed with SW620 cells untreated in Opti-MEM™ culture medium for 24 h. Colocalization images were constructed using the Colocalization Threshold tool, indicating areas of green and blue fluorescence signal overlapping (grey).

Appendix 7

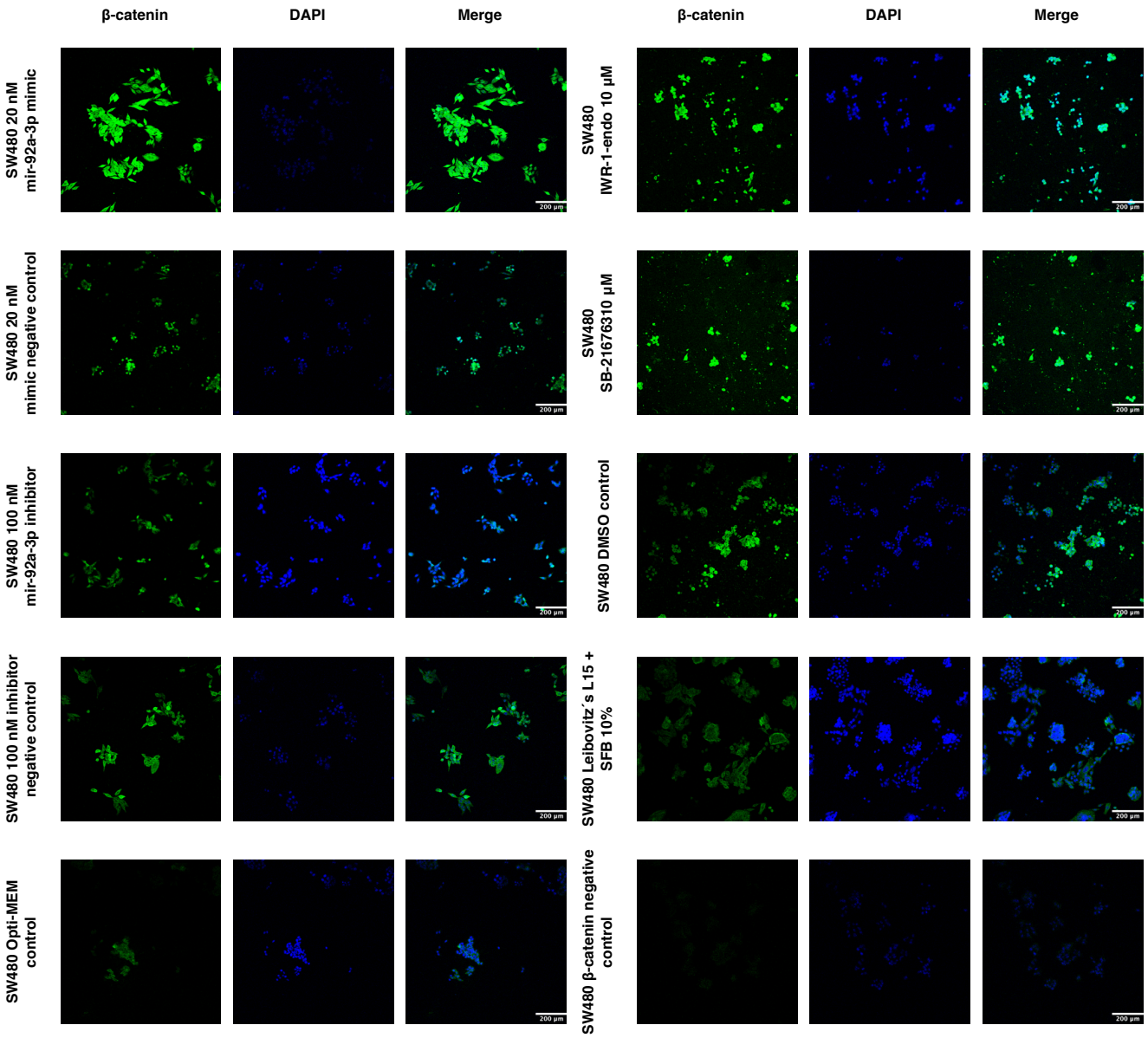

Appendix 7: Expression and β-catenin cellular localization in response to miR-92a-3p in sw480 cells (10X magnification): sw480 cells were transfected with miR-92a-3p mimic oligonucleotide 20 nM, miR-92a-3p inhibitor 100 nM, transfected with their corresponding negative control oligonucleotides, or in parallel were treated with IWR-1-endo 10 µM, SB-216763 10 µM, DMSO 0.81 µL/mL, or maintained untreated in Opti-MEM™ or Leibovitz´s L15 + SFB 10% for 24 hours, and then fixed and examined by immunofluorescence for β-catenin (green), and DAPI (blue) for the nuclei as reference.

Appendix 8

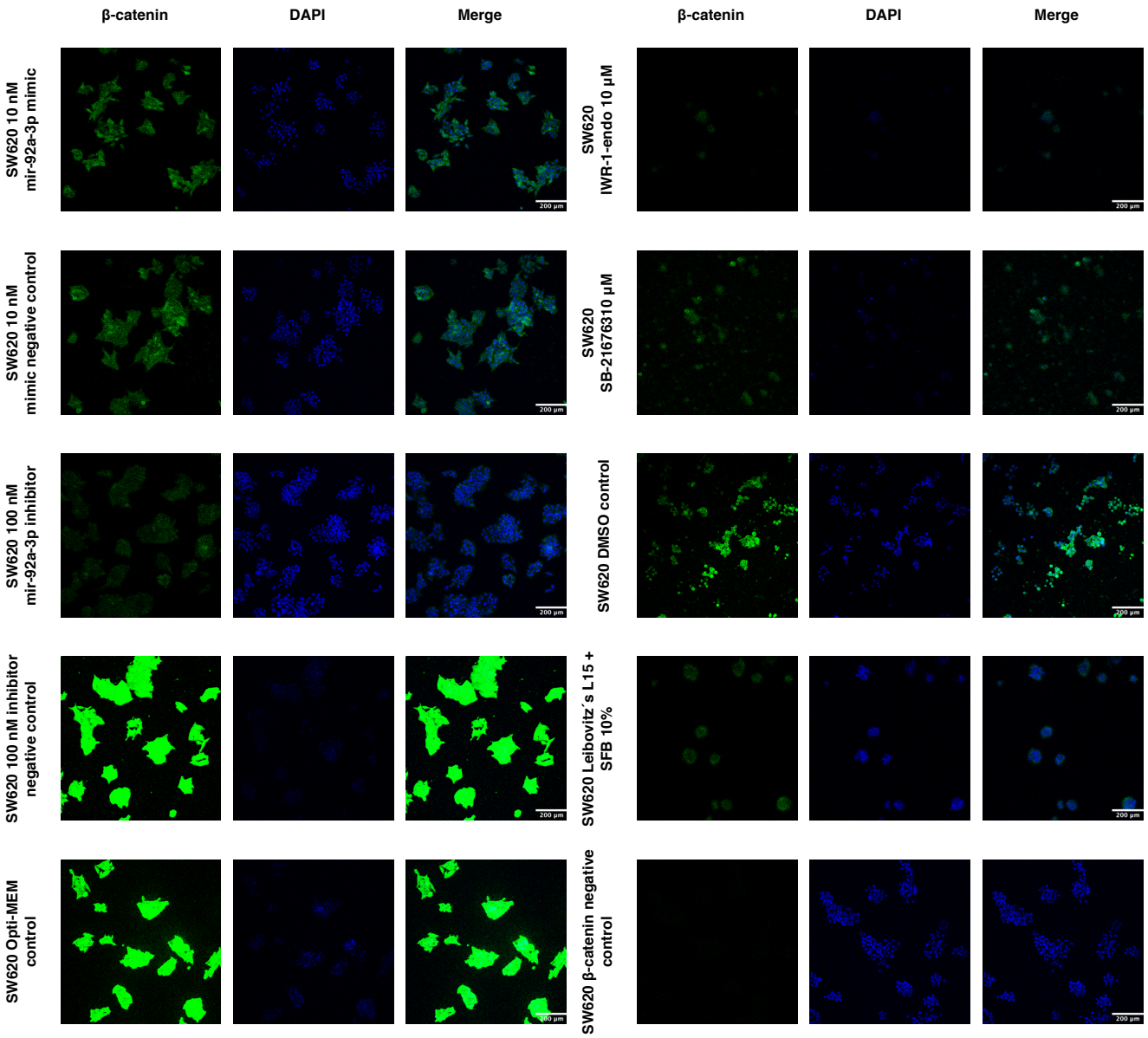

Appendix 8: Expression and β-catenin cellular localization in response to miR-92a-3p in sw620 cells (10X magnification): sw620 cells were transfected with miR-92a-3p mimic oligonucleotide 20 nM, miR-92a-3p inhibitor 100 nM, transfected with their corresponding negative control oligonucleotides, or in parallel were treated with IWR-1-endo 10 µM, SB-216763 10 µM, DMSO 0.81 µL/mL, or maintained untreated in Opti-MEM™ or Leibovitz´s L15 + SFB 10% for 24 hours, and then fixed and examined by immunofluorescence for β-catenin (green), and DAPI (blue) for the nuclei as reference.

Appendix 9

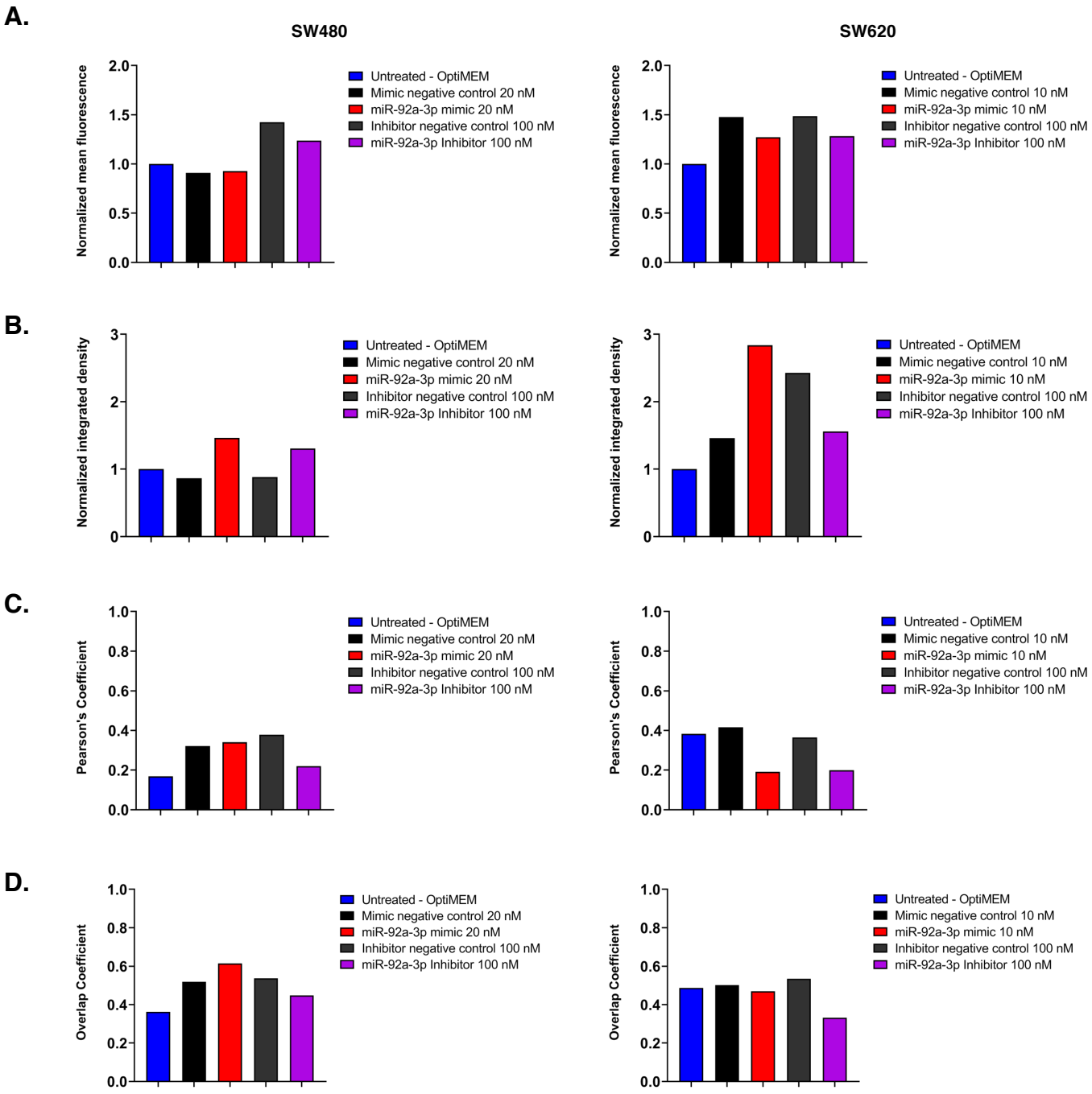

Appendix 9: Semiquantitative analysis of β-catenin in response to miR-92a-3p in SW480 and SW620 cells: Normalized mean fluorescence **(A)**, normalized integrated density **(B)**, Pearson's colocalization coefficient **(C)**, and overlapping coefficient **(D)** of SW480 and SW620 cells immunofluorescence images presented in Figure 8. Colocalization images were constructed using the Colocalization Threshold tool, indicating areas of green and blue fluorescence signal overlapping (grey). Pearson's and Overlap coefficients of the presented images were obtained using the JACoP tool (Just Another Colocalization Plugin), as a form of semiquantitative analysis of blue and green signal colocalization. Higher Pearson's and Overlap coefficients indicate increased colocalization of blue and green fluorescence. Data represent the results of the images presented in Figure 6 (n=1).

Appendix 10

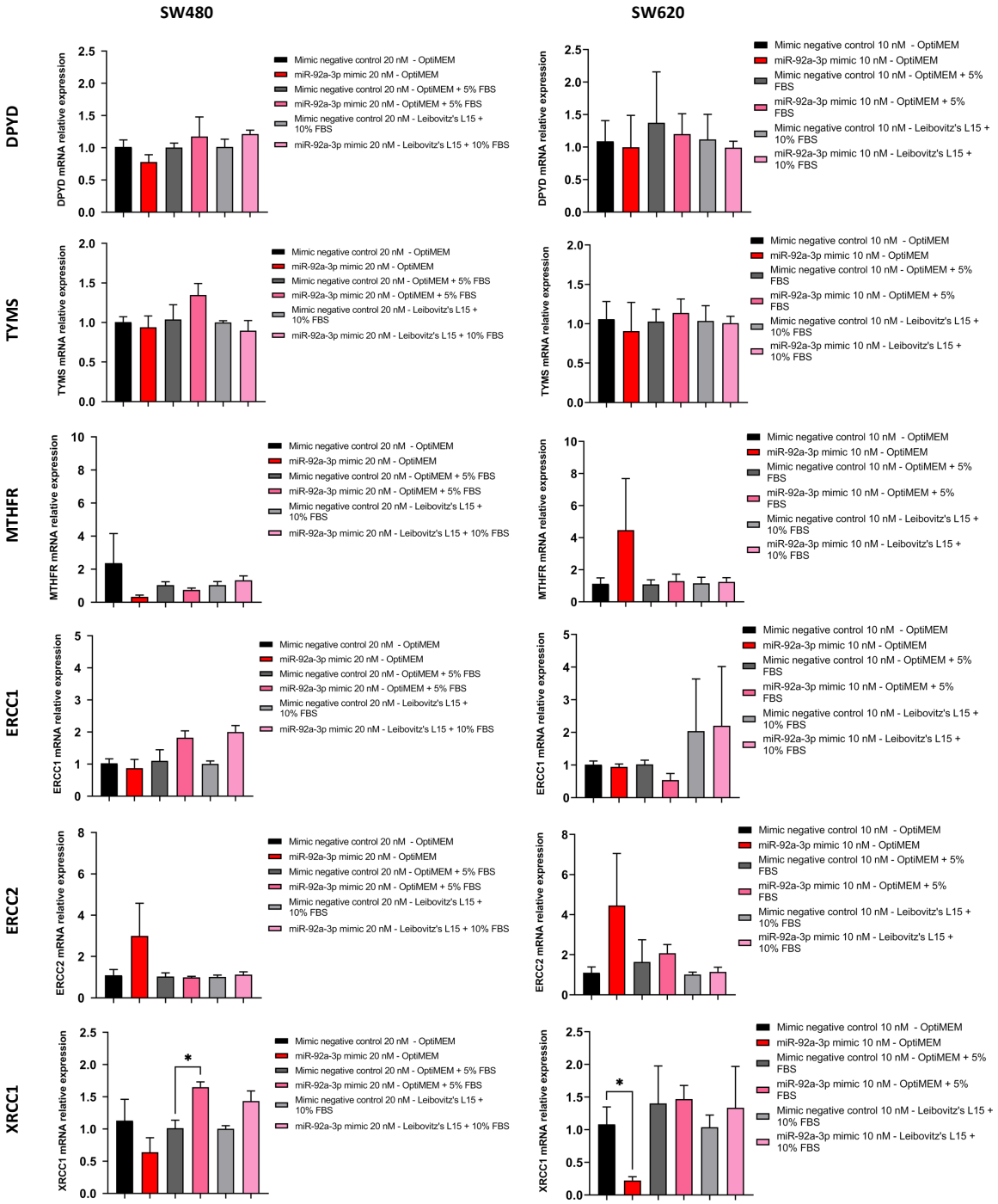

Appendix 10. Expression of genes associated with 5-FU and L-OHP response in SW480 and SW620 cell lines transfected with miR-92a-3p-mimic or inhibitors in supplemented culture medium: RT-qPCR analysis showing the relative expression of *DPYD*, *TYMS*, *MTHFR*, *ERCC1*, *ERCC2*, and *XRCC1* mRNA upon miR-92a-3p mimic transfection in SW480 and SW620 cells under three different conditions: transfection with unsupplemented Opti-MEM™; transfection with Opti-MEM™ supplemented with 5% FBS 5 hours after transfection; or transfection with miR-92a-3p-mimic using Opti-MEM™ followed by change of culture medium to Leibovitz's L-15 supplemented with 10% FBS 5 hours after. Statistical differences in mRNA levels were determined using the Mann-Whitney U test (*p=0.05). Data represent the means ± SEM from three independent experiments.

Appendix 11

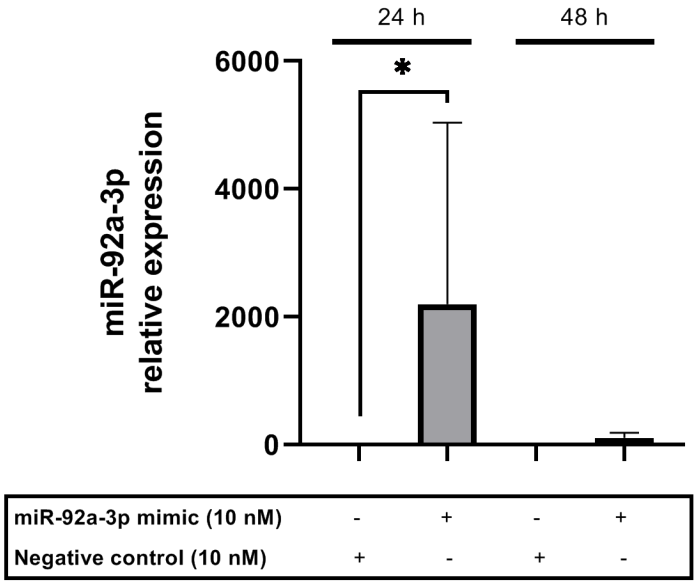

Appendix 11. Transfection efficiency curve in SW620 cell lines transfected with miR-92a-3p oligonucleotides: **(A)** RT-qPCR analysis comparing the relative expression of miR-92a-3p in SW620 cells transfected with increasing concentrations of mimic or negative control after 24 and 48 hours. Statistical differences in miR levels were determined using the Mann-Whitney U test (*p=0.05). Data represent the means ± SEM from three (24 h) and two (48 h) independent experiments.